

The magnetic soil, derived from ancient alluvium, is richer in iron than the less magnetic soil. This can be seen in EDX data, which shows iron to be the second most abundant element (after silicon) in the silt and clay fraction of the magnetic soil, and the third (after silicon and aluminum) in the nonmagnetic soil. The only difference between the two soil histories seems to be the influence of the alluvium. Therefore, the increased iron content of the magnetic soil may be the product of iron concentration due to water table fluctuation (precipitation of dissolved iron at the redox boundary) near an ancient river, or of weathering of minerals carried by a river from the mountains. Of the ancient alluvium soils, Lietzke et al. (1989) stated that the iron oxide distribution and soil color did not support the hypothesis of long periods of water table fluctuation. In light of this it seems more likely that sediments deposited by the river caused the increase in iron content not actions of a fluctuating, river-influenced water table.

Figure 17 shows ancient alluviums on Copper Ridge and relatively absent from the Chestnut ridge. Copper Ridge also shows a higher density of magnetic bull's-eyes. This again points to the ancient alluviums and soils derived from them as the source of the magnetic anomalies. Precise correlation between the magnetic anomalies and the alluviums is not seen for two reasons. Firstly, the magnetic signal is a function of the thickness of the magnetically susceptible soil. Some mapped alluviums may be too thin to be anomalously magnetic. Secondly

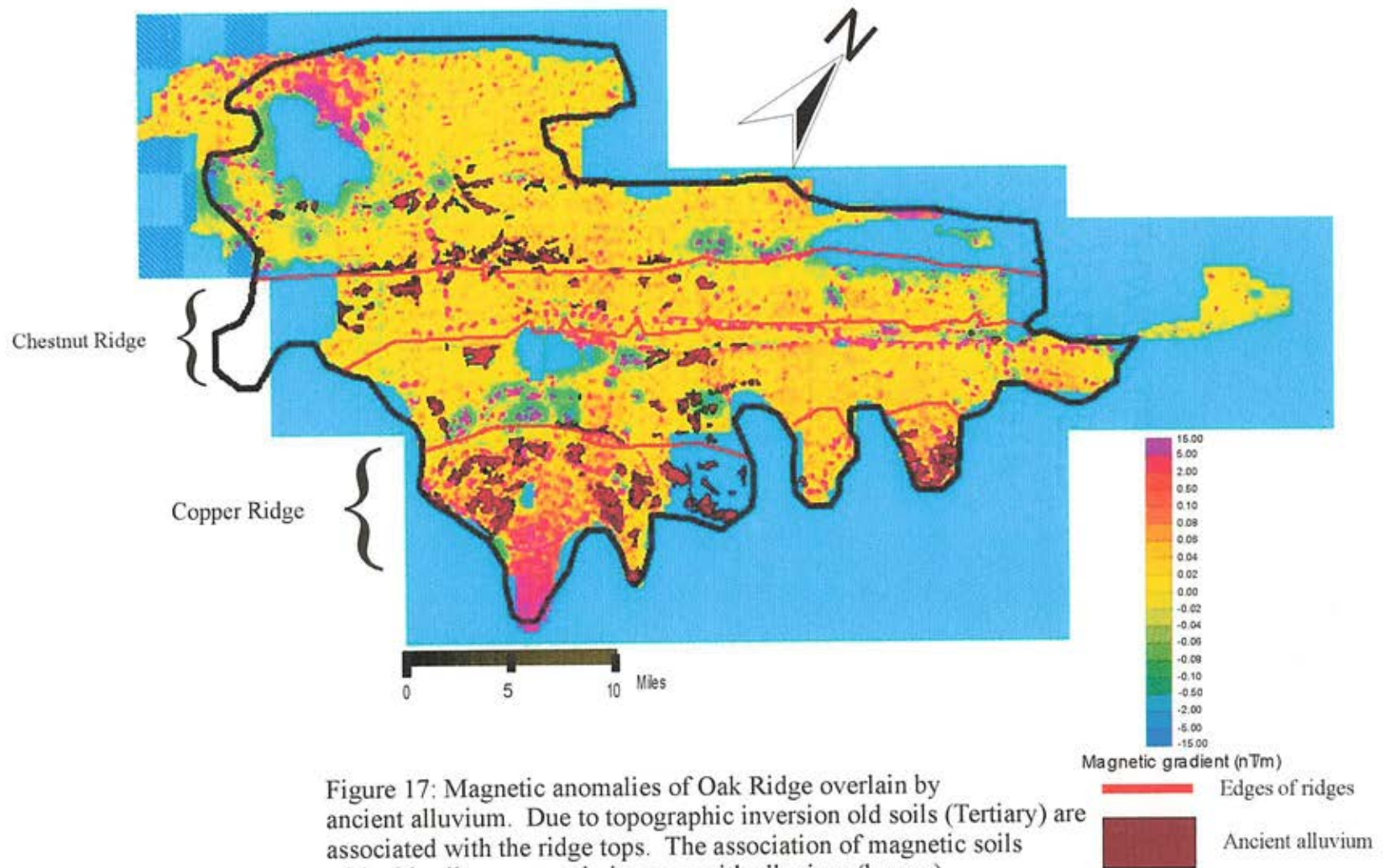


Figure 17: Magnetic anomalies of Oak Ridge overlain by ancient alluvium. Due to topographic inversion old soils (Tertiary) are associated with the ridge tops. The association of magnetic soils with old soils occurs only in areas with alluvium (brown).

them as the source of the magnetic anomalies. Precise correlation between the magnetic anomalies and the alluviums is not seen for two reasons. Firstly, the magnetic signal is a function of the thickness of the magnetically susceptible soil. Some mapped alluviums may be too thin to be anomalously magnetic. Secondly, soils derived from the alluviums may underlie other soils, creating an anomaly associated with a non-alluvium-mapped soil.

The Influence of Karst

When water reaches the dolomite bedrock its flow is “confined to cracks and joints” (Lietzke, 1994). The flow of water through the rock dissolves the carbonate, enlarging the fractures and eventually creating dolines. The joint system on Copper Ridge is oriented perpendicular and parallel to the strike of the ridge (Hatcher et al., 1992). The dolines on Copper Ridge, shown in Figure 13, also strike perpendicular and parallel to ridge strike reflecting the orientation of the joint set from which they formed. Dr. William Doll correlated magnetic anomalies to low lying areas on Copper Ridge (Figure 13). The magnetically anomalous regions reflect the deposition of iron rich colluvium or alluvium derived from ancient alluviums into low-lying dolines, which act as sediment traps. The transformation of the iron in the soil to maghemite through redox cycles continued after deposition as evidenced by the soil profiles that show susceptibility spikes at relict A/C→Bw horizon. Magnetization of the soil might be a function of hydromorphy (water fluctuation) in the doline, helping to explain magnetic soil association with dolines. The dolines may also allow for packages

of magnetic soils to become thick enough to be detected by airborne magnetometers.

Conclusions

Anaerobic microbial Fe reduction followed by formation of maghemite ($\gamma\text{Fe}_2\text{O}_3$), or abiological weathering of the Fe(III) bearing minerals followed by oxidation leading to maghemite, are the two mechanisms which best explain the high magnetic susceptibility of some soils on the ORR. The magnetic soil recovered from inside anomaly B rests in a doline and is rich in iron relative to the soil recovered outside the anomaly. The greater iron content allowed for greater production of maghemite. The major source of iron in the soil recovered inside anomaly B was ancient alluvium that was deposited in the doline from higher elevations of Copper Ridge. The iron found in the ancient alluviums is a product minerals that weathered after being transported by an ancient river. Magnetic anomalies found to be associated with dolines on Copper ridge may be a function of hydromorphy inside the dolines allowing for greater maghemite crystallization or of the greater thickness of the magnetic soils within the doline.

Implications and Recommendations for Further Work

The ability to distinguish anthropogenic objects such as buried drums and unexploded ordinance from magnetic soil using an aerial survey will never be absolute. However, conclusions offered by my study may help.

When looking for anthropogenic anomalies within the boundary of the ORR itself, priority should be given to anomalies not associated with soils

mapped as ancient alluviums, as these anomalies are likely to be the result of maghemite concentration in the soils. If certainty is needed as to whether an anomaly associated with ancient alluviums is anthropogenic, walkover magnetometry should be employed. If the signal obtained during a walkover reflects a large number of narrow anomalies (distinct points), this is likely the result of buried objects. If the survey yields a small number of broad anomalies (Figure 11) it is probable that the magnetic source is magnetic soil.

Outside of the ORR, distinction between anthropogenic anomalies and magnetic soils becomes more difficult. Soil maps should be inspected when interpreting magnetic data, particularly in regions of high precipitation, because magnetic soils are found most often associated with these wet climates (Singer and Fine, 1989). Furthermore, if at any site anomalies are found to reflect some regional geologic trend, as with the fracture sets on Copper Ridge, investigators should inspect some of the anomalies to look for a connection between the cause of such an anomaly and the trend. In this way, a small number of inspections could furnish insight into a large number of anomalies.

Further work is necessary in order to classify the soils that were removed from magnetic anomaly B, and understand the relationship between duration of pedogenesis and magnetic susceptibility. Base saturation levels and a complete particle size analysis should be performed on the soils. Carbon 14 age dating should be performed on the organic material found in the buried A-horizons to look for correlation between duration of pedogenesis and magnetic susceptibility.

Finally, computer modeling of the airborne magnetic data may be useful to evaluate the influence of the highly magnetic upper soil horizons on the magnetic signal. This will help determine whether thin layers highly of magnetic soil create a strong signal or if we need thickened soils as found in the karst terrain of the ORR.

BIBLIOGRAPHY

- Birkeland, P.W., 1999, *Soils and Geomorphology*: Oxford, Oxford University Press, 430 p.
- Crownover, S. H., Collins, M. E., and Lietzke, D. A., 1994, Parent materials and stratigraphy of a doline in the Valley and Ridge Province: *Soil Science Society of America Journal*, v. 58, p. 1738-1746.
- Doll, W. E., Nyquist, J. E., Beard, L. P., and Gamey, T. J., 2000, Airborne geophysical surveying for hazardous waste site characterization on the Oak Ridge Reservation, Tennessee: *Geophysics*, v. 65, p. 1372-1387.
- Dearing, J. A., Hay, L. K., Baban, S. M. J., Huddleston, A. S., Wellington, E. M. H., and Loveland, P. J., 1996, Magnetic susceptibility of soil: an evaluation of conflicting theories using a national data set: *Geophys. J. Int.*, v. 127, p. 728-734.
- Devouard, B., Posfał, M., Hua, H., Bazyłinski, D. A., Frankel, R. B., and Buesk, P. R., 1998, Magnetite from magnetotactic bacteria: Size distributions and twinning: *American Mineralogist*, v. 83, p. 1387-1398.
- Doll, W. E., Helm, J. M., and Beard, L. P., 1995, Airborne detection of magnetic anomalies associated with soils on the Oak Ridge Reservation, Tennessee, *Symposium on the Applications of Geophysics to Engineering and Environmental Problems*: Eng. Environ. Geophys. Soc., p. 619-626.
- Doll, W. E., Nyquist, J. E., Beard, L. P., and Gamey, J. T., 2000, Airborne geophysical surveying for hazardous waste site characterization on the Oak Ridge Reservation, Tennessee: *Geophysics*, v. 65, p.1372-1387.
- Drumm, E. C., Kane, W. F., Kettle, R. H., Ben-Hassine, J., Scarborough, J. A., 1990, Subsidence of residual soils in a karst terrain: ORNL/TM-11525, 92 p.
- Dunlap D. J., Ozdemir O., 1997, *Rock Magnetism Fundamentals and Frontiers*: New York, Cambridge University Press, 573 p.
- Fassbinder, J. W. E., Stanjek, H., and Vali, H., 1990, Occurrence of magnetic bacteria in soil: *Nature*, v. 343, p. 161-163.
- Gifford, A. C., 1999, Clay soil fulgarites in the Eastern Goldfields of Western Australia: *Journal of the Royal Society of Western Australia*, v. 82, p. 165-168.

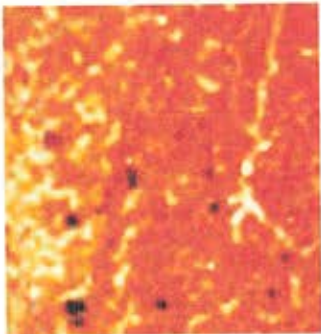
- Halliday, D., Resnick, R., and Walker, J., 1997, *Fundamentals of Physics Extended*: New York, John Wiley and Sons Inc., 1142 p.
- Hatcher, R.D., Lemiszki P.J., Dreier R.B., Ketelle R.H., Lee R.R., Leitzke D.A., McMaster W.M., Foreman J.L., and Lee S.Y., 1992, Status report on the geology of the Oak Ridge Reservation, ORNL/TM-12074, 244 p.
- Helm, J., 1995, Magnetic susceptibility study of bedrock and selected soils, Oak Ridge Reservation, TN, to be released as ORNL ES/ER report.
- Jackson, M. L., 1975, *Soil Chemical Analysis-Advanced Course*. 2nd ed.: Published by author, Department of Soil Science, University of Wisconsin, Madison, WI., 895 p.
- King, A. M., Jones, A. M., Dorling, S. R., Merefield, J. R., Stone, I. M., Hall, K., Garner, D. V., Hall, P. A., and Stokes, B., 1999, Study for particulate sampling, sizing and analysis for composition: ETSU N/01/00049/REP, 131 p.
- Kopp, O.C., and Lee, S.Y., 1987, An unusual occurrence of maghemite on soils developed on dolostones of the Knox Group, Oak Ridge, Tennessee, *in* Proceedings of the International Clay Conference, Denver, The Clay Minerals Society, Bloomington, IN, p. 205-211.
- Lee, S.Y., Kopp, O.C. and Lietzke, D.A., 1984, Mineralogical characterization of West Chestnut Ridge soils: ORNL/TM-9361, 85 p.
- Leitzke, D. A., 1994, Soils of Walker Branch Watershed: ORNL/TM-11606, 107 p.
- Lietzke, D. A., Ketelle, R. H., and Lee, R. R., 1989, Soils and Geomorphology of the East Chestnut Ridge Site: ORNL/TM-11364, 45 p.
- Lovley, D. R., 1990, Magnetite formation during microbial dissimilatory iron reduction: *in* Iron Biominerals, R. B. Frankel and H. P. Blakemore, eds., New York, Plenum Press, p. 151-166.
- Maher, B. A., and Taylor, R.M., 1988, Formation of ultrafine-grained magnetite in soils: *Nature*, v. 336, p. 368-370.
- Moukarika, A., O'Brien, F., Coey, J. M. D., and Resende, Mauro, 1991, Development of magnetic soil from ferroan dolomite: *Geophysical Research Letters*, v. 18, p. 2043-2046.
- Mullins, C. E., 1977, Magnetic susceptibility of the soil and its significance in soil science, a review: *Journal of Soil Science*, v. 28, p. 223-246.

- Munsell Soil Color Charts, 2000, New Windsor, NY, GretagMacbeth.
- Nyquist, J. E. and Doll, W. E., 1996, Analysis and interpretation of airborne geophysical data acquired over the Melton Valley waste area groupings and adjacent areas, Oak Ridge National Laboratory, Oak Ridge, Tennessee: ES/ER/TM-208, 113 p.
- Phillips, D. H., Ammons, J. T., Lee, S. Y., and Lietzke, D. A., 1998, Deep weathering of calcareous sedimentary rock and the redistribution of iron and manganese in soil and saprolite: *Soil Science of America*, v. 163, p. 71-81.
- Reynolds, J.M., 1997, *An Introduction to Applied and Environmental Geophysics*: New York, John Wiley and Sons, 796 p.
- Ruhe, R. V., Olson, C., G., 1980, Soil welding: *Soil Science*, v. 130, p. 132-139.
- Schwertmann, U., and Taylor, R. M., 1977, Iron oxides: in *Minerals in Soil Environments*, J. B. Dixon and S. B. Weed, eds., *Soil Science of America*, Madison, p. 145-180.
- Singer, M. J., and Fine, P., 1989, Pedogenic factors affecting magnetic susceptibility of Northern Californian soils: *Soil Science of America*, v. 53, p. 1119-1127.
- Soil survey staff, 1975, *Soil Taxonomy*, U.S. Dept. of Agriculture Handbook, no. 436, 754 p.
- Solomon, D. K., Moore, G. K., Toran, L. E., Dreier, R. B., and McMaster, W. M., 1992, *Status Report: A hydrologic framework for the Oak Ridge Reservation*: ORNL/TM-12026, 95 p.
- Stanjek, H., Fassbinder, J. W. E., Vali, H., and Graf, W., 1994, Evidence of biogenic greigite: *Journal of Soil Science*, v. 45, p. 97-103.
- Tarbuck, E. J., and Lutgens, F.K., *Earth: An Introduction to Physical Geology*: Upper Saddle Rivers, Prentice Hall, 670 p.
- Taylor, M. R., Maher, B. A., and Self, P. G., 1987, Magnetite in soils: I. The synthesis of single-domain and superparamagnetic magnetite: *Clay Minerals*, v. 22, p. 411-422.
- Taylor, R. M., and Schwertmann, U., 1974, Maghemite in soils and its origin: I. Properties and observations on soil maghemites: *Clay Minerals*, v. 10, p. 289-310.

Tompson, R., and Oldfield, F., 1986, Environmental magnetism: London, Allen and Unwin, 227 p.

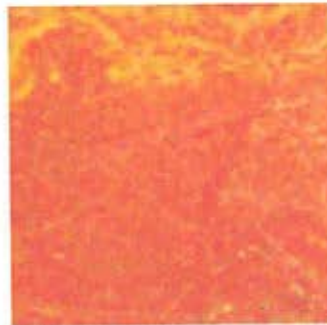
Plate 1

16



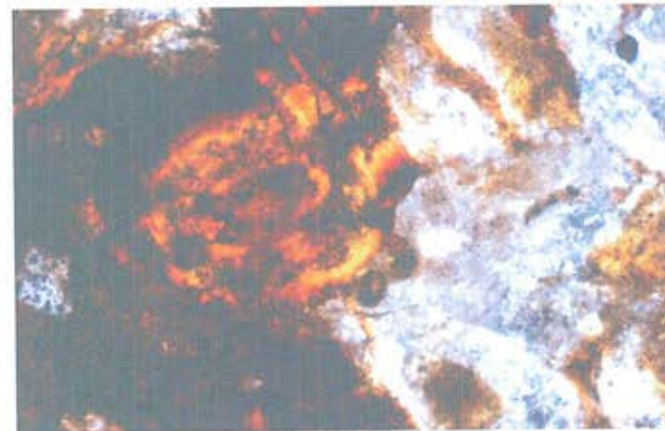
3 cm

Picture 1: Scanned thin section showing clay matrix of the magnetic core. Notice the large numbers of iron and manganese glaeubules (black).



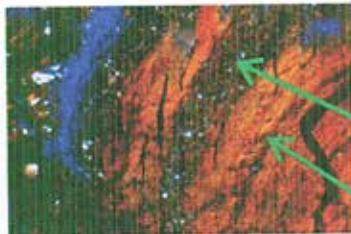
3 cm

Picture 2: Scanned thin section showing clay matrix of the non-magnetic core. The matrix has fewer iron glaeubules than the magnetic core and is lighter in color.



0.2 mm

Picture 3: Vosepic fabric in the Bw horizon from Profile 1 of the non-magnetic core. Aligned clay, evidence of translocation, is used to distinguish the nature of this horizon from a C horizon (unaltered parent material). Picture taken in cross-polarized light.

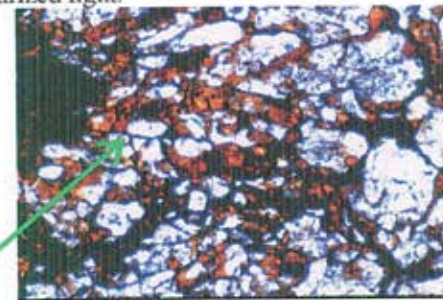


0.5 mm

Picture 4: Alternating siltans and argillans from a depth of 108 inches in the magnetic core. Siltans and argillans are evidence of translocation. Picture taken in cross-polarized light.

Siltan

Argillan

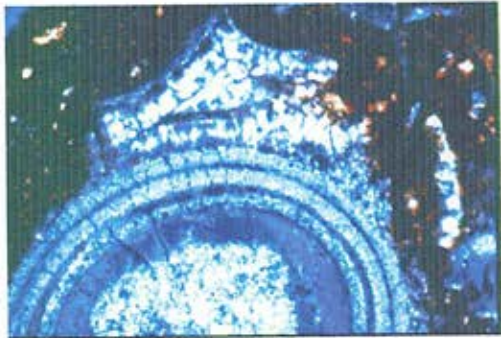


0.5 mm

Triple junction of quartz grains is a typical feature in metaquartzite.

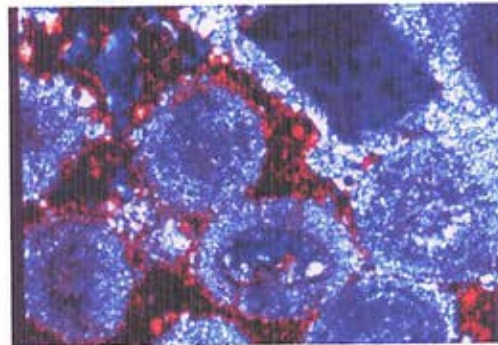
Picture 5: This quartzite from profile 2 C→B-horizon of the magnetic core is evidence of a non-dolomite parent material. Picture taken in plane-polarized light.

Plate 2



0.3 mm

Picture 1: Oolitic chert coated by iron oxide in cross-polarized light.



0.3 mm

Picture 2: Oolitic chert cemented with iron oxide in cross-polarized light.



3 cm

Picture 3: Grass stem and root found in a buried A-horizon.



Picture 4: Rounded magnetic particle composed of pure iron oxide based on EDX (Figure A3.3).

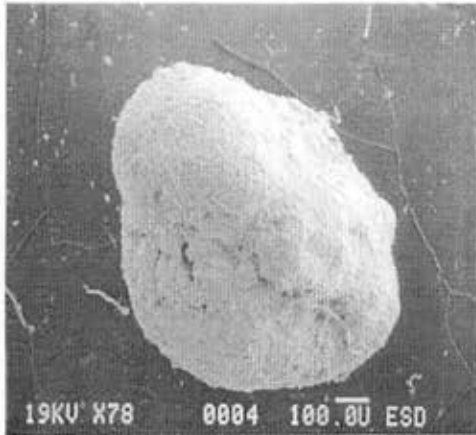


Picture 5: Large rounded iron oxide-dominated particle from profile 3, A-horizon. This particle is more than 1000 μm across.

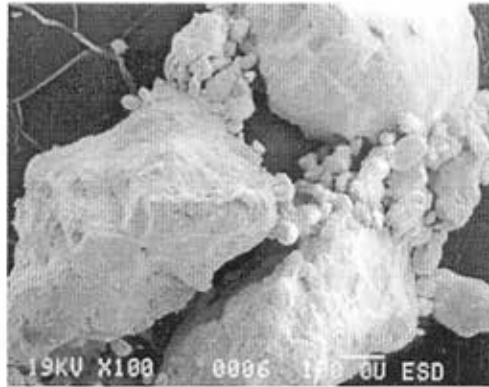


Picture 6: Maghemite particle from 39 ft level in the magnetic core.

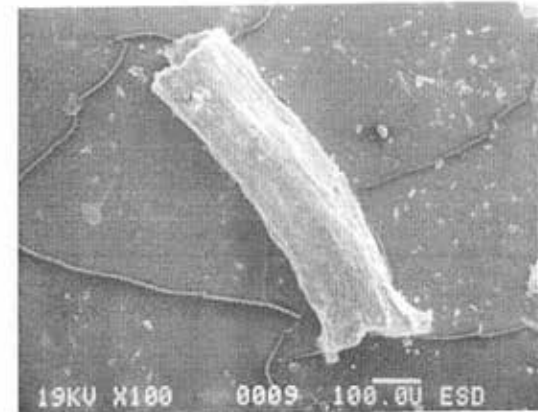
Plate 3



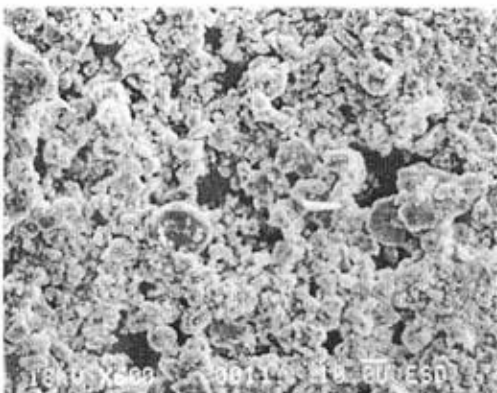
Picture 1: Si-rich particle from bulk soil removed from Profile 1, A-horizon.



Picture 2: Fe-rich particles from Profile 2, A-horizon.



Picture 3: Root removed from nonmagnetic core. See EDX (Appendix 3.10)



Picture 4: Silt and clay fraction from the magnetic core.

APPENDICES

APPENDIX 1: DIAGRAMS OF ANOMALY B SOIL CORE WITH MAGNETIC SUSCEPTIBILITIES

Figure A1.1: Composite diagram of cores extracted within the magnetic anomaly showing horizon changes and magnetic susceptibility	96
Figure A1.2: Diagram of the first (top) core tube extracted within magnetic anomaly showing horizon changes and magnetic susceptibility	97
Figure A1.3: Diagram of the second core tube extracted within magnetic anomaly showing horizon changes and magnetic susceptibility	98
Figure A1.4: Diagram of the third core tube extracted within magnetic anomaly showing horizon changes and magnetic susceptibility	99
Figure A1.5: Diagram of the fourth core tube extracted within magnetic anomaly showing horizon changes and magnetic susceptibility	100
Figure A1.6: Diagram of the fifth core tube extracted within magnetic anomaly showing horizon changes and magnetic susceptibility	101
Figure A1.7: Composite diagram of cores extracted outside of the magnetic anomaly showing horizon changes and magnetic susceptibility	102
Figure A1.8: Diagram of the first (top) core tube extracted outside of the magnetic anomaly showing horizon changes and magnetic susceptibility	103

Figure A1.9: Diagram of the second core tube extracted outside of the magnetic anomaly showing horizon changes and magnetic susceptibility	104
Figure A1.10: Diagram of the third core tube extracted outside of the magnetic anomaly showing horizon changes and magnetic susceptibility.	105
Figure A1.11: Appendix 1 legend.....	106

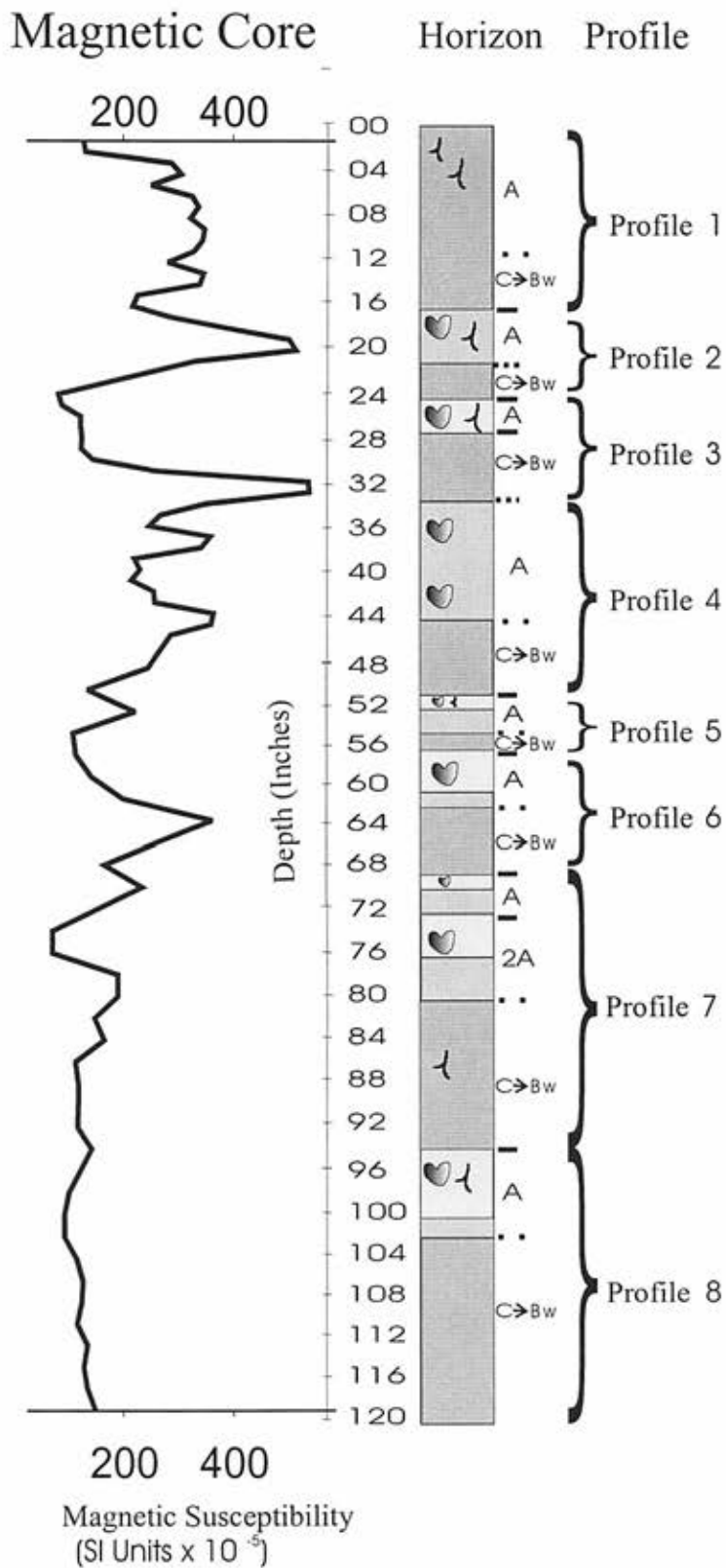


Figure A1.1: Composite diagram of cores extracted within the magnetic anomaly B showing horizon changes and magnetic susceptibility See Figure A1.11 for legend.

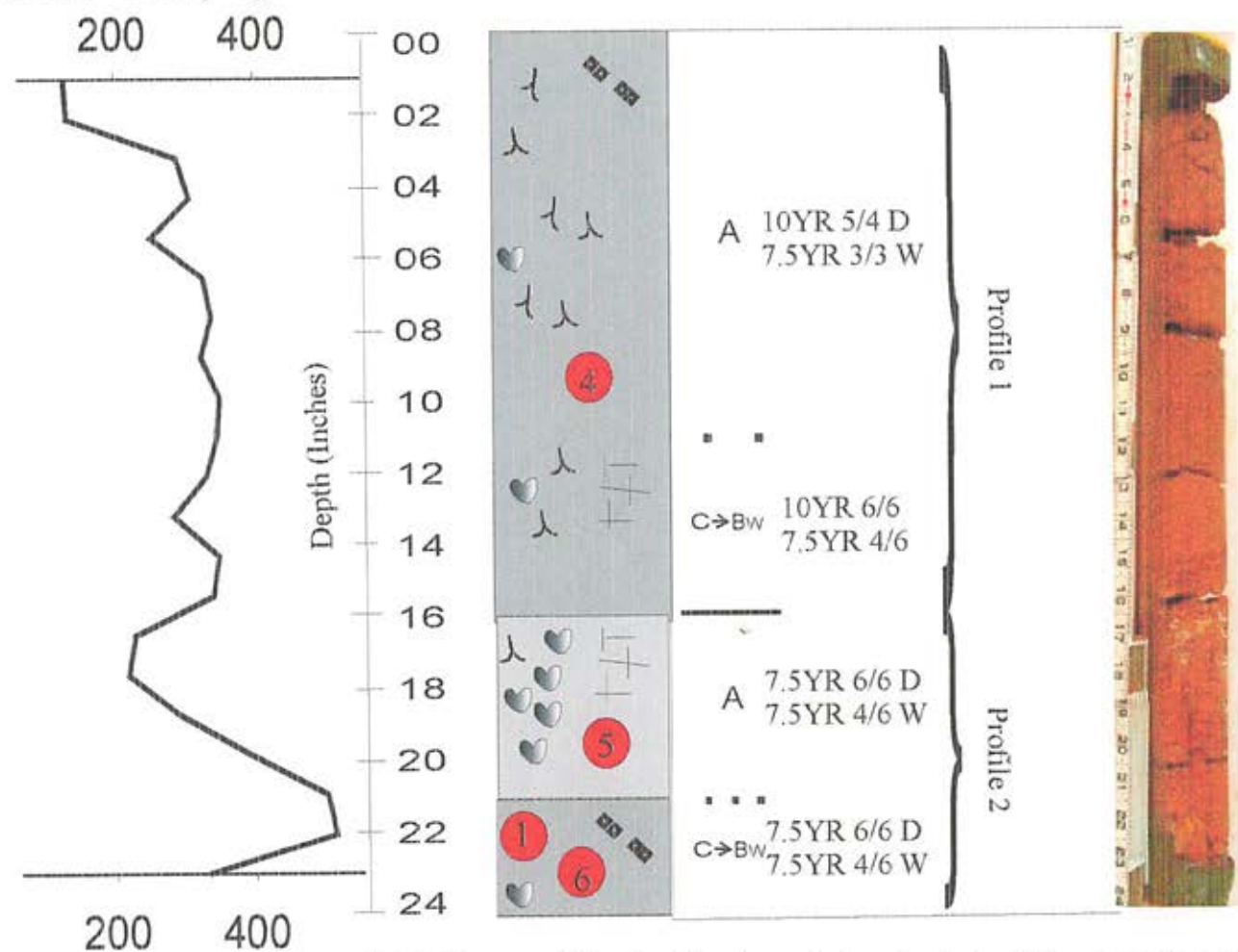
Handwritten text, mostly illegible due to extreme fading and bleed-through from the reverse side of the page. The text appears to be organized into several paragraphs or sections, but the specific words and sentences cannot be discerned.

At the bottom of the page, there is a line of text that appears to be a signature or a date, but it is also illegible due to fading.

Magnetic Core 028 (#1)

Horizon Color Profile

Picture



Magnetic Susceptibility
(S.I. Units x 10⁻³)

Figure A1.2: Diagram of the first (top) core tube extracted within magnetic anomaly B showing horizon changes and magnetic susceptibility. See Figure A1.11 for legend.

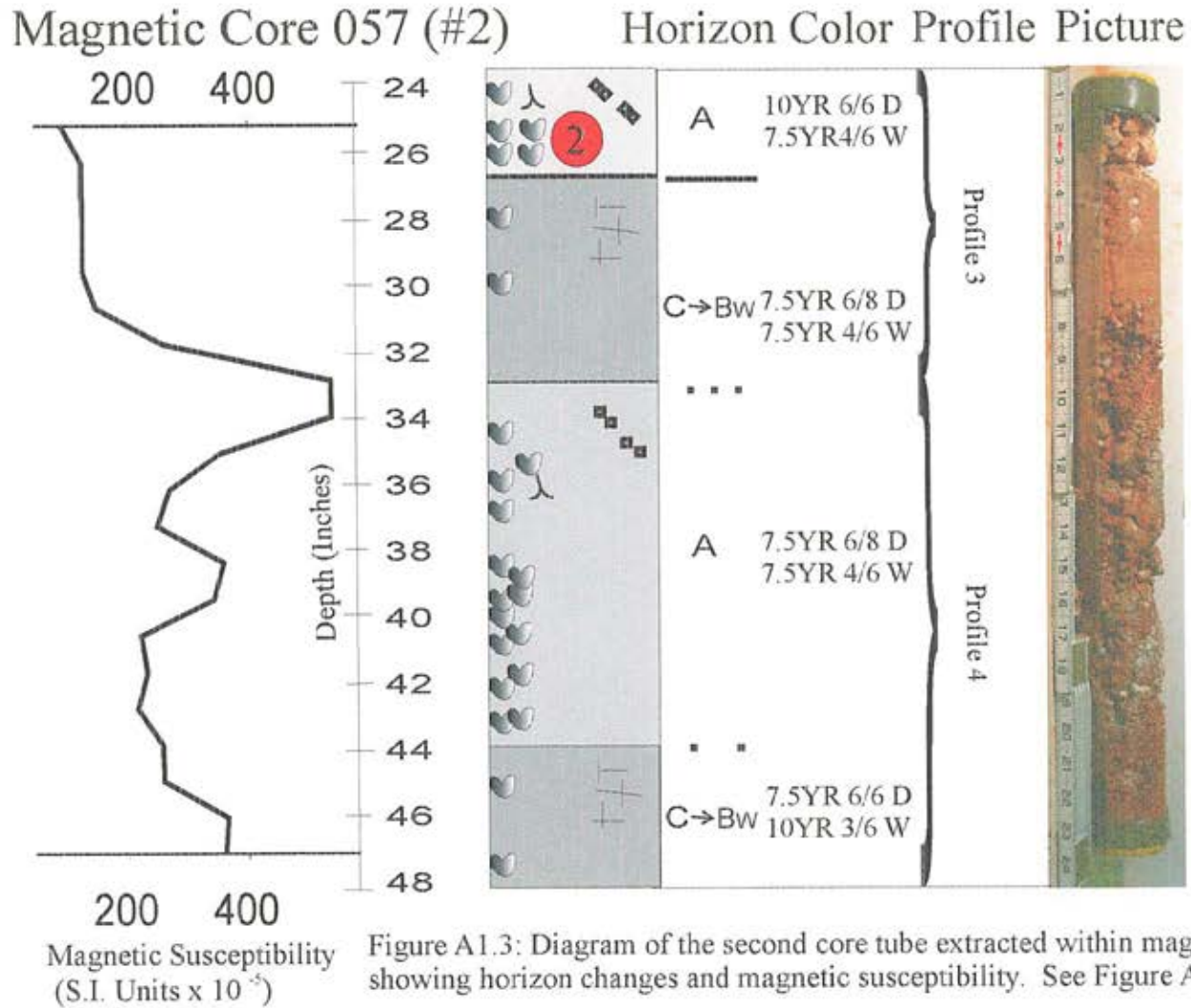


Figure A1.3: Diagram of the second core tube extracted within magnetic anomaly B showing horizon changes and magnetic susceptibility. See Figure A1.11 for legend.

Magnetic Core 082 (#3)

Horizon Color Profile Picture

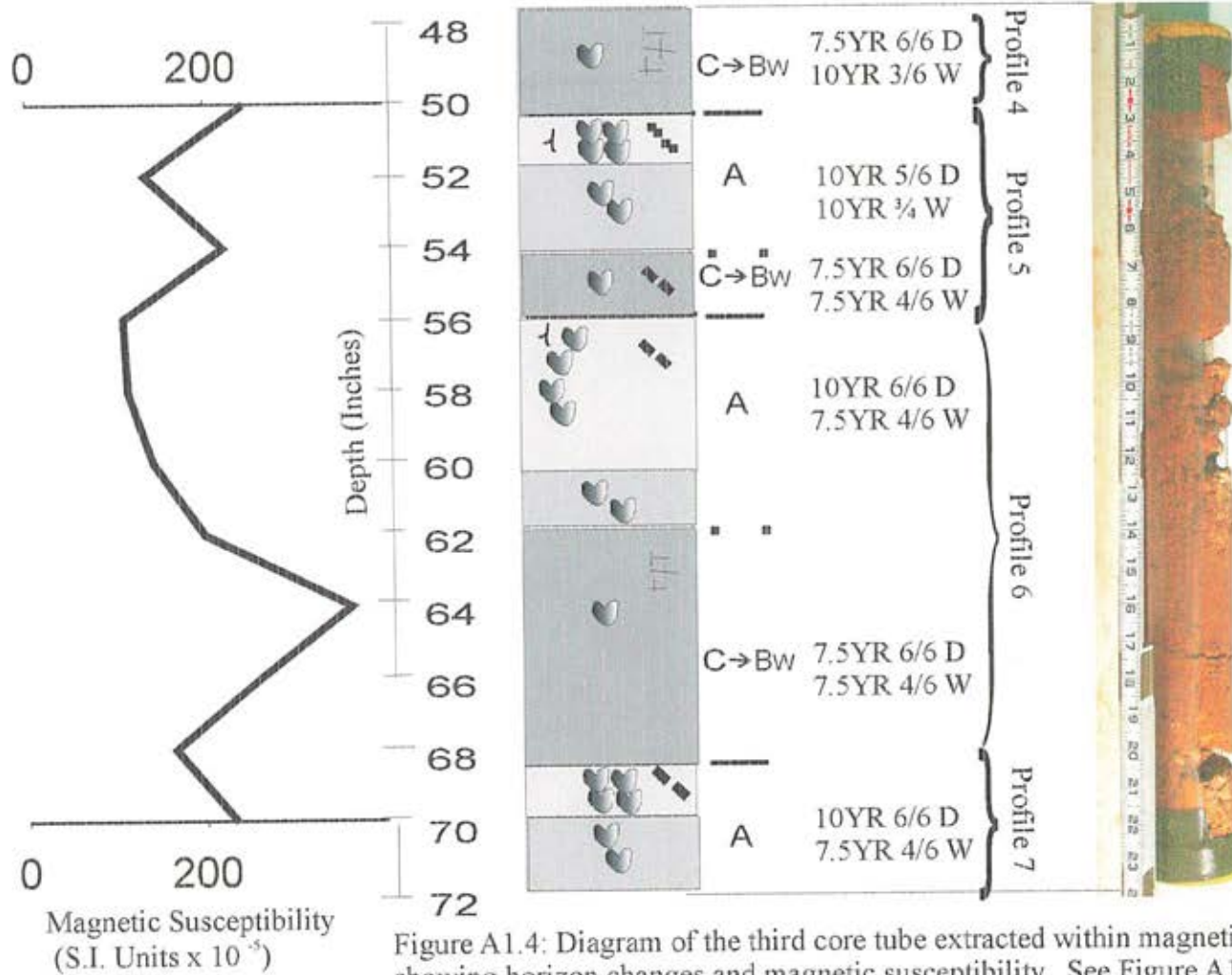
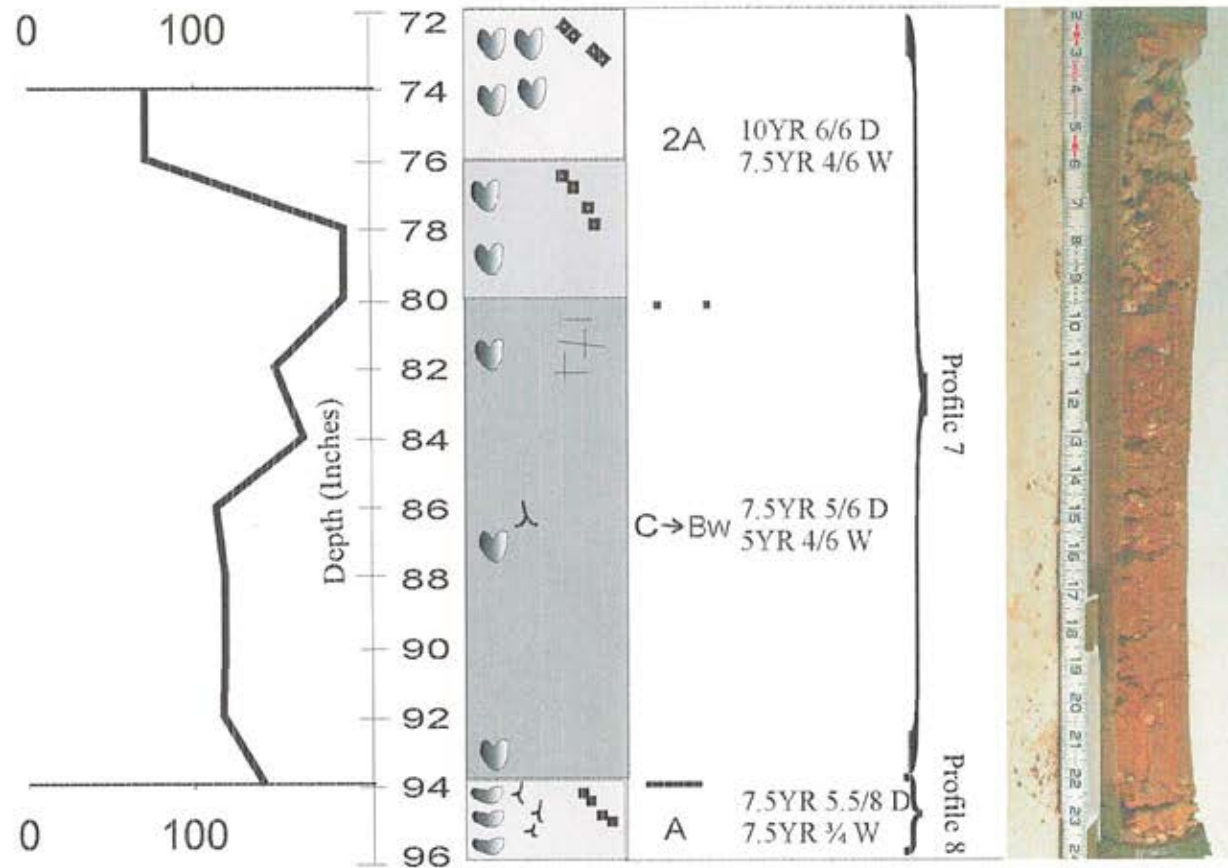


Figure A1.4: Diagram of the third core tube extracted within magnetic anomaly B showing horizon changes and magnetic susceptibility. See Figure A1.11 for legend.

Magnetic Core 110 (#4)

Horizon Color Profile Picture

100



Magnetic Susceptibility (S.I. Units x 10⁻⁵)

Figure A1.5: Diagram of the fourth core tube extracted within magnetic anomaly B showing horizon changes and magnetic susceptibility. See Figure A1.11 for legend.

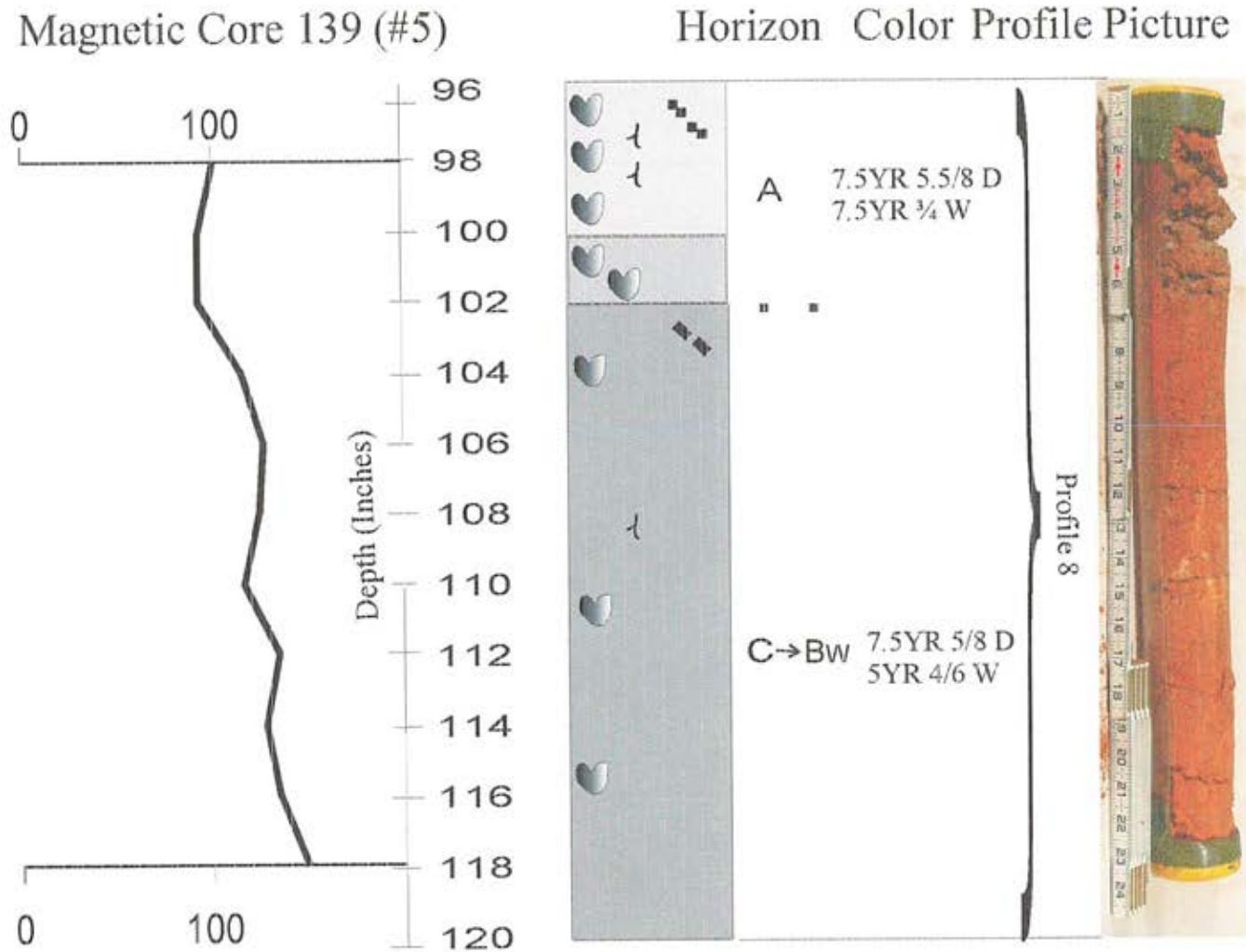


Figure A1.6: Diagram of the fifth core tube extracted within magnetic anomaly B showing horizon changes and magnetic susceptibility. See Figure A1.11 for legend.

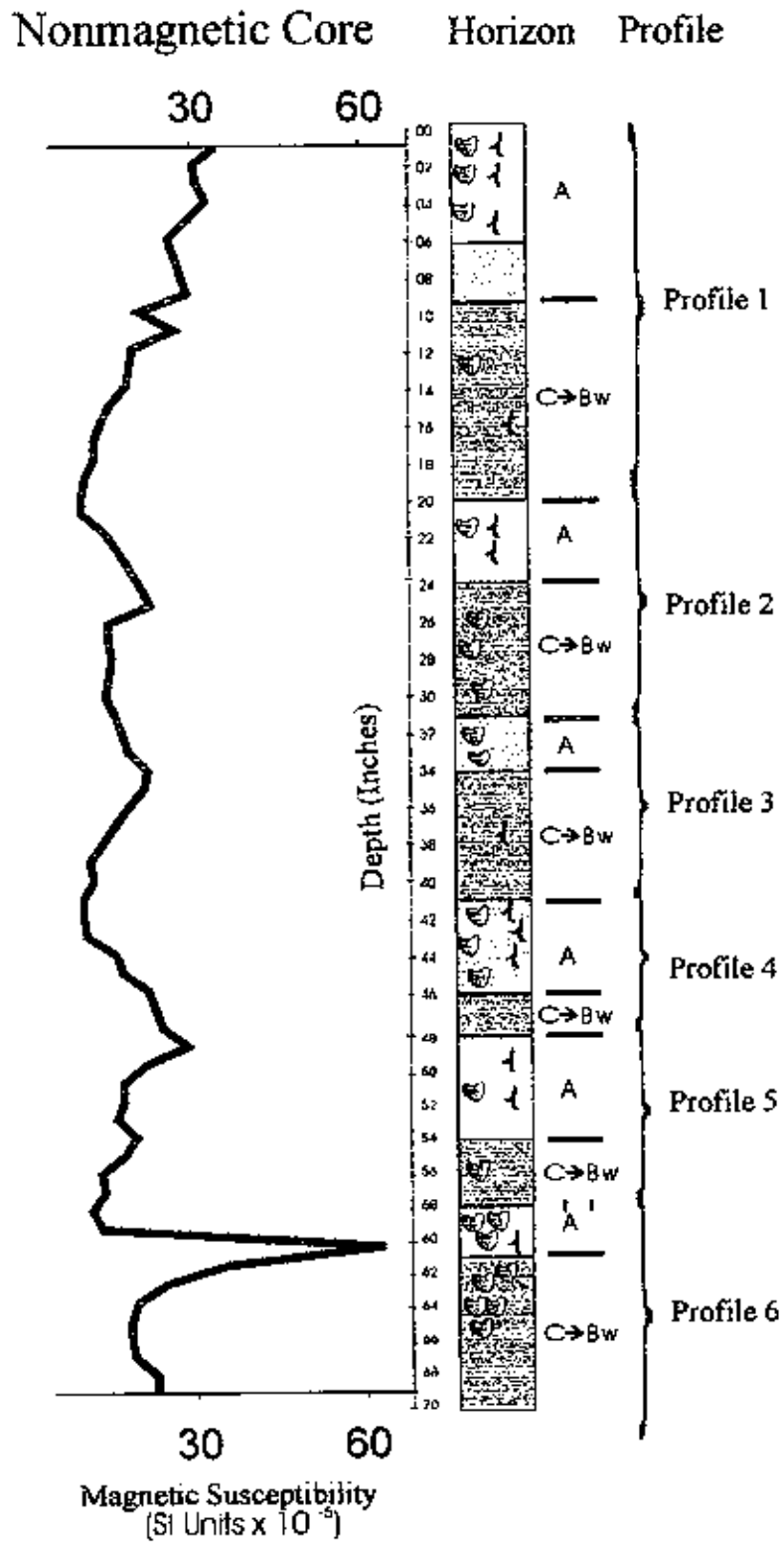
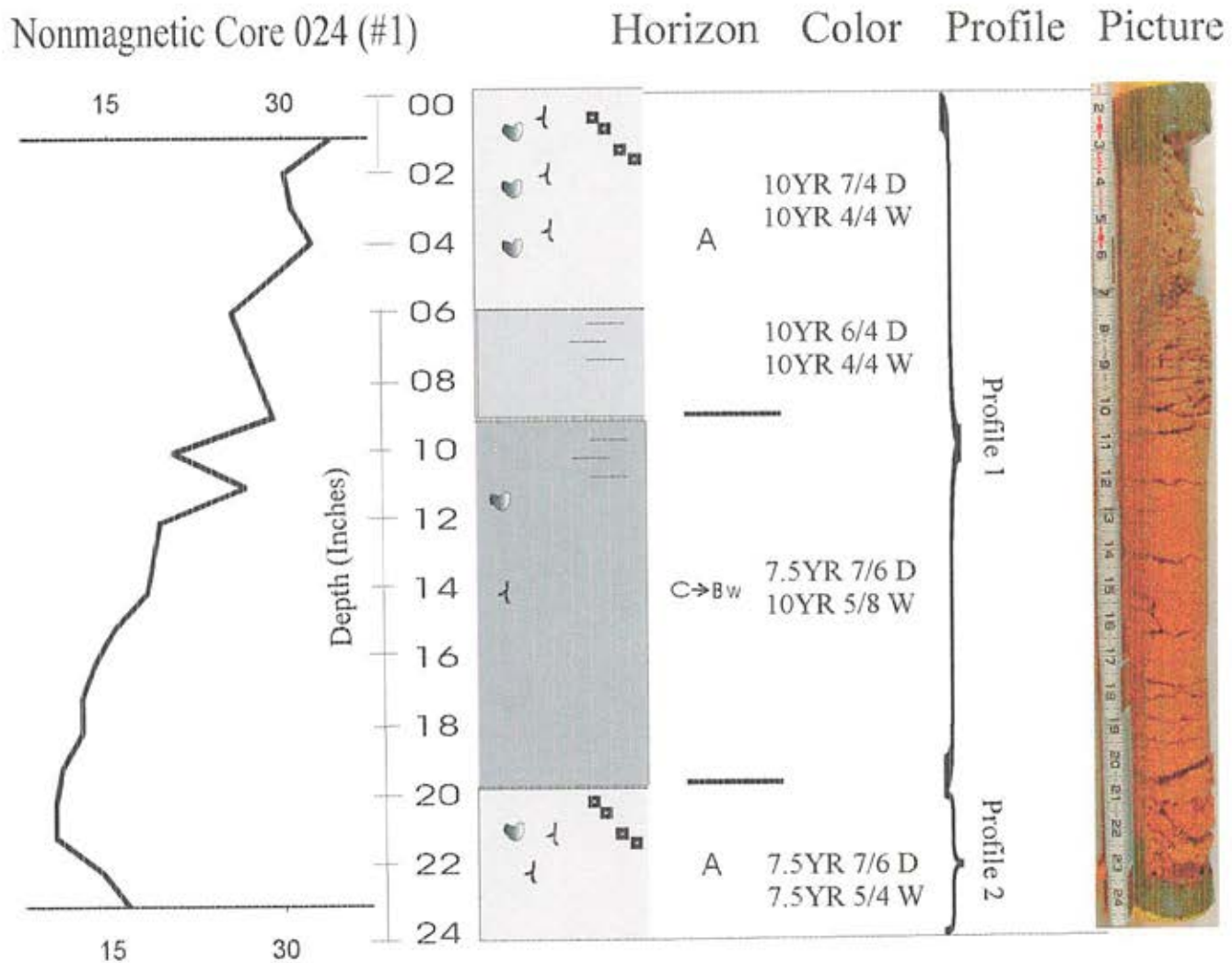
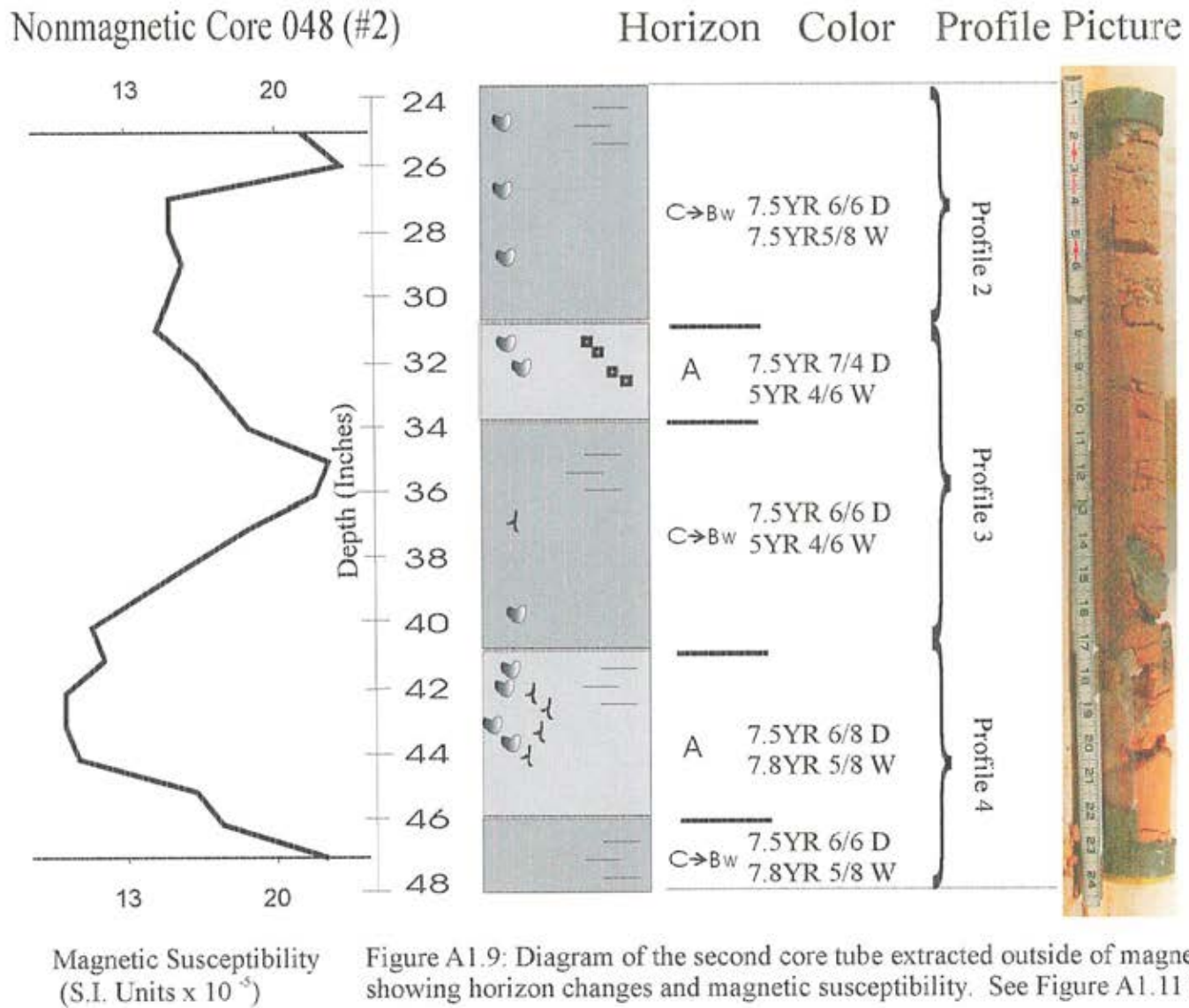


Figure A1.7: Composite diagram of cores extracted outside of the magnetic anomaly B showing horizon changes and magnetic susceptibility. See Figure A1.11 for legend.



Magnetic Susceptibility
(S.I. Units x 10⁻⁵)

Figure A1.8: Diagram of the first (top) core tube extracted outside of the magnetic anomaly B showing horizon changes and magnetic susceptibility. See Figure A1.11 for legend.



Nonmagnetic Core 070 (#3)

Horizon Color Profile Picture

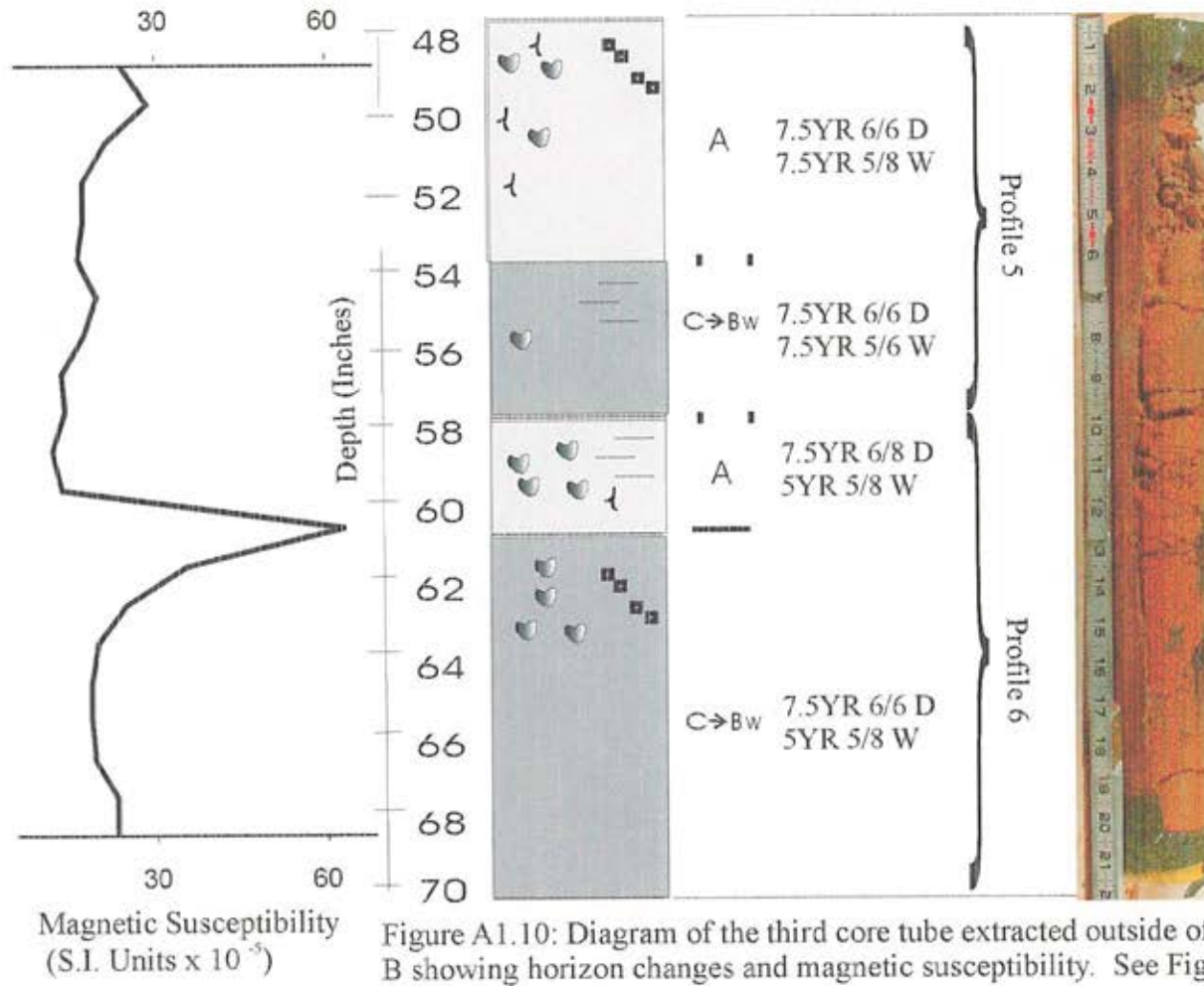
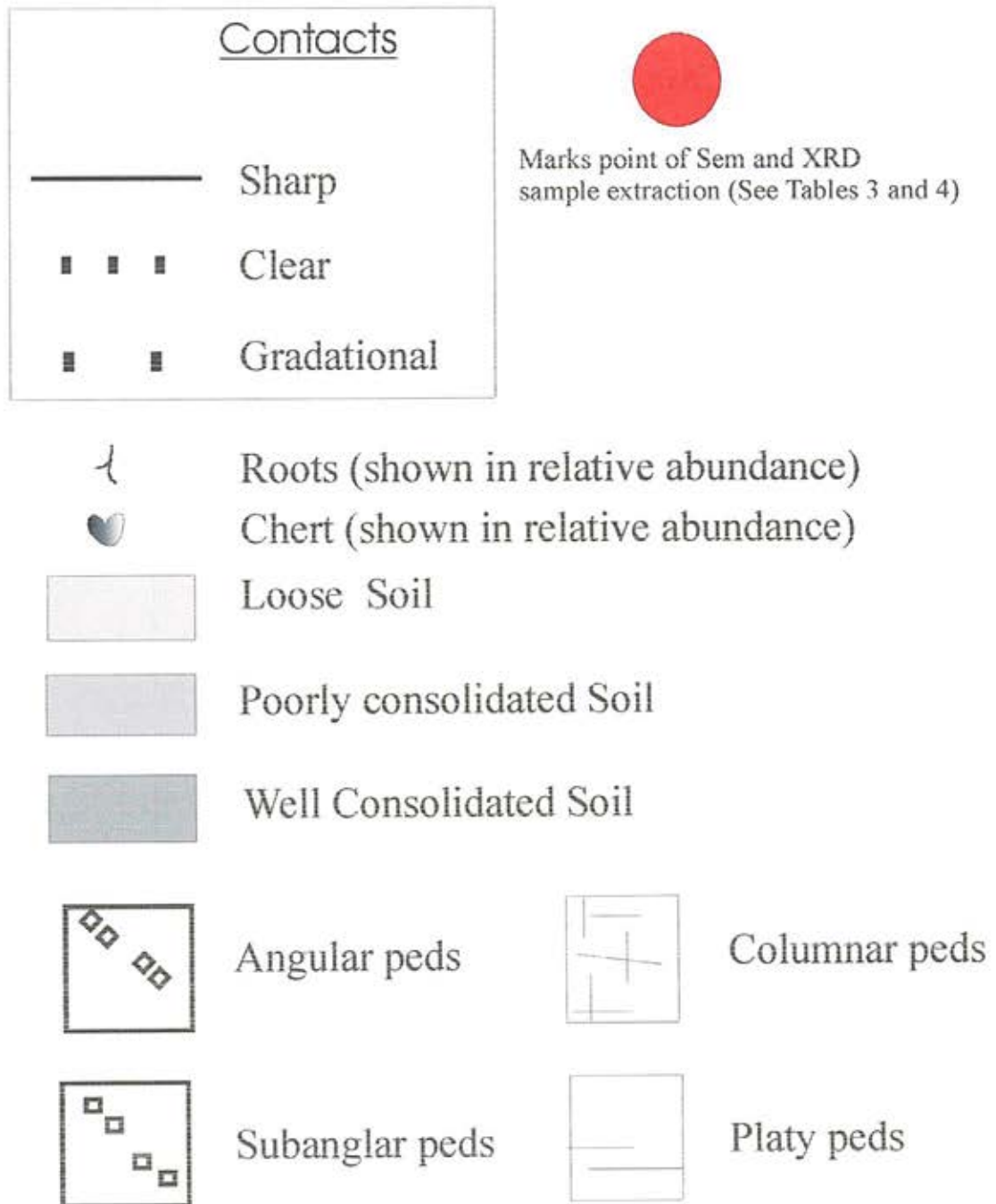


Figure A1.10: Diagram of the third core tube extracted outside of the magnetic anomaly B showing horizon changes and magnetic susceptibility. See Figure A1.11 for legend.

Appendix A Legend



Munsell Colors shown in wet (W) and dry (D)

Figure A1.11 Appendix 1 legend

APPENDIX 2: HORIZON DESCRIPTION DATA

Table A2.1 Horizon description data for magnetic core..... 108

Table A2.2 Horizon description data for non-magnetic core 113

Interval (In)	Profile	Horizon	Color	Texture and Consistence	Minerals	Peds	Roots	Boundary
0-11	1	A	10YR5/ 4 Dry 7.5YR 3/3 Wet	Silty clay, hard	Minor amounts of chert (<5%). Iron oxide glaebules are observed in thin section. The thin section shows chert to be impregnated with iron oxides. There is no evidence of clay infills.	Well developed fine (1-2 cm) columnar peds breaking down to angular blocky	Pervasive	Gradual
11-16	1	C→Bw	10YR6/ 6 Dry 7.5YR 4/6 Wet	Silty clay, hard	Minor amounts of chert (< 10%). Iron oxide glaebules are observed throughout and seen in thin section. The thin section shows chert to be impregnated with iron oxides. There is no evidence of clay infills.	Fine to Medium (.5 - 2 cm) angular blocky	Common	Sharp
16-21	2	A	7.5YR6/ 6 Dry 7.5YR 4/6 Wet	Sandy clay loam, loose	Large chert fragments (>1 cm across) added to smaller chert fragments make up 35% of the upper portion of the horizon and 25% of the lower. Most are iron oxide or manganese oxide stained or impregnated. Small (mm scale) angular to rounded quartz fragments found throughout. Charcoal colored iron oxide and manganese oxide stains and glaebules can be seen in hand sample as well as thin section.	Well developed fine (1-2cm) columnar peds breaking down to angular blocky	Grass can be seen at top of horizon	Clear
21-24	2	C→Bw	7.5YR6/ 6 Dry 7.5YR 4/6 Wet	Clay loam, hard	Small (mm scale) angular iron oxide stained chert (15%) and quartz dispersed through horizon. Iron oxide glaebules clearly seen in thin section.	Fine to Medium (0.5 - 2 cm) angular blocky	None	Sharp

Table A2.1 Horizon description data for magnetic core

Interval (In)	Profile	Horizon	Color	Texture and Consistence	Minerals	Peds	Roots	Boundary
24-27	3	A	10YR 6/6 Dry/ 7.5YR 4/6 Wet	Chert Cobble, very loose. Clay adheres to chert	Chert makes up 80% of this horizon. Fragments .01-2 cm. Chert is often iron oxide coated. Quartz is a minor constituent. Silty clay matrix adheres to some chert fragments.	Soil matrix adheres to chert fragments (angular)	Grass found in horizon	Sharp
27-33	3	C→Bw	7.5YR6/ 8 Dry 7.5YR 4/6 Wet	Clay loam, hard	Small (1 mm or less) chert, fragments are prevalent at the top of this horizon becoming less so with depth. Total chert <20% and some fragments are iron oxide coated.	Well developed fine (1-2cm) columnar peds breaking down to angular blocky (friable)	None	Clear
33-44	4	A	7.5YR6/ 8 Dry 7.5YR 4/6 Wet	Clay loam, loose	Large chert fragments (up to 6 cm across) added to smaller chert fragments make up 30-40% of the horizon. Many are iron oxide or manganese oxide stained or impregnated and some are weathering to kaolinite. Small (mm scale) angular to rounded quartz fragments are also found throughout the horizon. Iron oxide stains observed and a very large (3 cm across) manganese oxide nodule was found. Iron oxide concretions found in thin section as well.	Fine to Medlum (.5 - 2 cm) subangular blocky	Found in thin section only	Gradual

Table A2.1 Horizon description data for magnetic core (cont.)

Interval (In)	Profile	Horizon	Color	Texture and Consistence	Minerals	Peds	Roots	Boundary
44-51	4	C→Bw	7.5YR 6/6 Dry 10YR 3/6 Wet	Clay loam, hard	Quartz and chert found dispersed in horizon 1-10 mm in size (<20%). The chert is iron oxide impregnated and includes a magnetic fragment. In thin section the inner part of the magnetic fragment was rust-red color-stained and nonmagnetic. The outer part was black and impregnated with a magnetic oxide. The chert itself is oolitic.	Well developed fine (1-2cm) columnar peds breaking down to angular blocky (friable)	None	Sharp
51-54	5	A	10YR 5/6 Dry 10YR 3/4 Wet	Silty clay, loose at top to poorly consolidated at bottom	Chert common (1-2 cm) makes up 25-30% of horizon. Fine magnetic particles extractable from matrix (0.1-1 mm)	Fine to Medium (0.5 - 2 cm) subangular blocky	Roots found (probably grass)	Gradual
54-56	5	C→Bw	7.5YR 6/6 Dry 7.5YR 4/6 Wet	Silty clay, Hard	Chert fragments (0.5 cm) dispersed in horizon (10-15%). Quartz grains and iron oxide glaeubules occur with less regularity than profile 5, A-horizon.	Fine to Medium (0.5 - 2 cm) angular blocky	None	Sharp
56-62	6	A	10YR 6/6 Dry 7.5YR 4/6 Wet	Silty clay, loose	Chert comprises 60-70% of the horizon and ranges in size from 0.1 mm - 2 cm. Quartz grains (<1 mm) are found throughout and iron oxide stains are common.	Mostly defined by chert but soil fragments are very fine (3 mm) angular blocky	Infrequent	Gradual

Table A2.1 Horizon description data for magnetic core (cont.)

Interval (In)	Profile	Horizon	Color	Texture and Consistence	Minerals	Peds	Roots	Boundary
62-69	6	C→Bw	7.5YR 6/6 Dry 7.5YR 4/6 Wet	Clay loam, hard	5-10% iron oxide chert (some are stained). Quartz not common above the sand size. Iron oxide staining observed on chert and matrix.	Very weak columnar breaking down to Fine to Medium (0.5 - 2 cm) angular blocky	None	Sharp
69-72	7	A	10YR 6/6 Dry 7.5YR 4/6 Wet	Silty clay, Poorly consolidated	35-35% Chert fragments, many iron oxide stained. Fragments range from 1 mm-3 cm scale. Mm size quartz a common constituent.	Fine to Medium (0.5 - 2 cm) angular blocky	None	Sharp
72-80	7	A2	10YR6/ 6 Dry 10YR 3/4 Wet	Silt Loam, very loose at top of horizon to poorly consolidated at bottom	40-45% chert fragments (up to 5 cm), many iron oxide coated. Sand size quartz also common.	Fine to Medium (0.5 - 2 cm) subangular blocky	None	Gradual
80-94	7	C→Bw	7.5YR 5/6 Dry 5YR 4/6 Wet	Clay loam, hard	10-15% chert (1 cm or smaller) often iron oxide coated. Iron oxide/ manganese oxide glaeboles seen in matrix. Some sand size quartz.	Columnar breaking down to medium (1 cm) subangular blocky	Infrequent	Sharp
94-102	8	A	7.5YR 5.5/8 Dry 7.5YR 3/4 Wet	Silty clay, loose at top to poorly consolidated at bottom	40-50% up to 3 cm iron oxide stained chert. Quartz also found (mm scale)	Fine to medium (0.5 - 2 cm) subangular blocky	Many roots found (probably grass)	Gradual

Table A2.1 Horizon description data for magnetic core (cont.)

Interval (In)	Profile	Horizon	Color	Texture and Consistence	Minerals	Peds	Roots	Boundary
102-120	8	C→Bw	7.5YR 5/8 Dry 5YR 4/6 Wet	Clay loam, hard	Chert (<20%) up to one cm with minor quartz and iron oxide or manganese oxide glæbules	Fine to medium (.5 - 2 cm) angular blocky	Infrequent	NA

Table A2.1 Horizon description data for magnetic core (cont.)

Interval (In)	Profile	Horizon	Color	Texture and Consistence	Minerals	Peds	Roots	Boundary
1--9	1	A	10YR 7/4 Dry 10YR 4/4 Wet changing to 10YR 6/4 Dry 10YR 4/4 Wet	Loose silty clay	1-2 mm chert common at top (20%) to rare at bottom (5%)	Very fine (1-5 mm) subangular blocky at top changing to medium Platy (2-5 mm) at 6 inch depth	Common	Sharp
9--20	1	C→Bw	7.5YR 7/6 Dry 10YR 5/8 Wet	Hard silty clay	Occasional 1-2 mm chert (<10%)	Weak platy breaking down to very fine subangular blocky (2-5 mm)	Occasional	Sharp
20-24	2	A	7.5YR 7/6 Dry 7.5YR 5/4 Wet	Loose silty clay	Occasional 1-2 mm chert (15%)	Small-medium (2-20 mm) subangular blocky	Common	Sharp
24-31	2	C→Bw	7.5 YR 6/6 Dry 7.5YR 5/8 Wet	Hard clay	Heavily kaolinized chert fragments, some coated with iron oxide (10%)	Platy breaking down to small-medium (2-10 mm) subangular blocky	None	Sharp
31-34	3	A	7.5YR 7/4 Dry 5YR 4/6 Wet	Loose clay loam	Heavily kaolinized chert fragments some coated with Mn oxide (15%)	Fine (5 mm) subangular blocky	None	Sharp
34-41	3	C→Bw	7.5YR 6/6 Dry 5YR 4/6 Wet	Hard clay	One large chert piece at 39 inches but rare otherwise (5%)	Platy breaking down to fine (5 mm) subangular blocky	Sparse plant matter	Sharp
41-46	4	A	7.5YR6/8 Dry 7.5YR 5/8 Wet	Loose clay loam	Chert common, some fresh, some kaolinized (15%)	Platy breaking down to fine subangular blocky (5-10 mm)	Plentiful, some appear clay filled	Sharp

Table A2.2 Horizon description data for non-magnetic core

Interval (In)	Profile	Horizon	Color	Texture and Consistency	Minerals	Peds	Roots	Boundary
46-48	4	C→Bw	7.5YR 6/6 Dry 5YR 5/8 Wet	Hard clay	None	Platy breaking down to medium (1-2 cm) subangular blocky	None	Sharp
48-54	5	A	7.5 YR 6/6 Dry 7.5YR 5/8 Wet	Loose silty clay	1 cm chert is uncommon (10%)	Fine angular blocky (5mm)	Grass (plentiful)	Gradual
54-58	5	C→Bw	7.5 YR 6/6 Dry 7.5YR 5/6 Wet	Hard silty clay	Small amounts of Mn oxide coated chert (5%)	Weak platy breaking down to fine subangular blocky (5mm)	None	Gradual
58-61	6	A	7.5YR6/8 Dry 5YR 5/8 Wet	Loose clay loam	Large chert (1-3 cm), dark and fresh (not kaolinized) (25%)	Medium platy (2-5 mm)	Sparse	Sharp
61-72	6	C→Bw	7.5YR6/6 Dry 5YR 5/8 Wet	Hard silty clay	Chert to 65 inches then absent (associated with Mn and Fe staining)	Medium (10mm) subangular blocky	None	

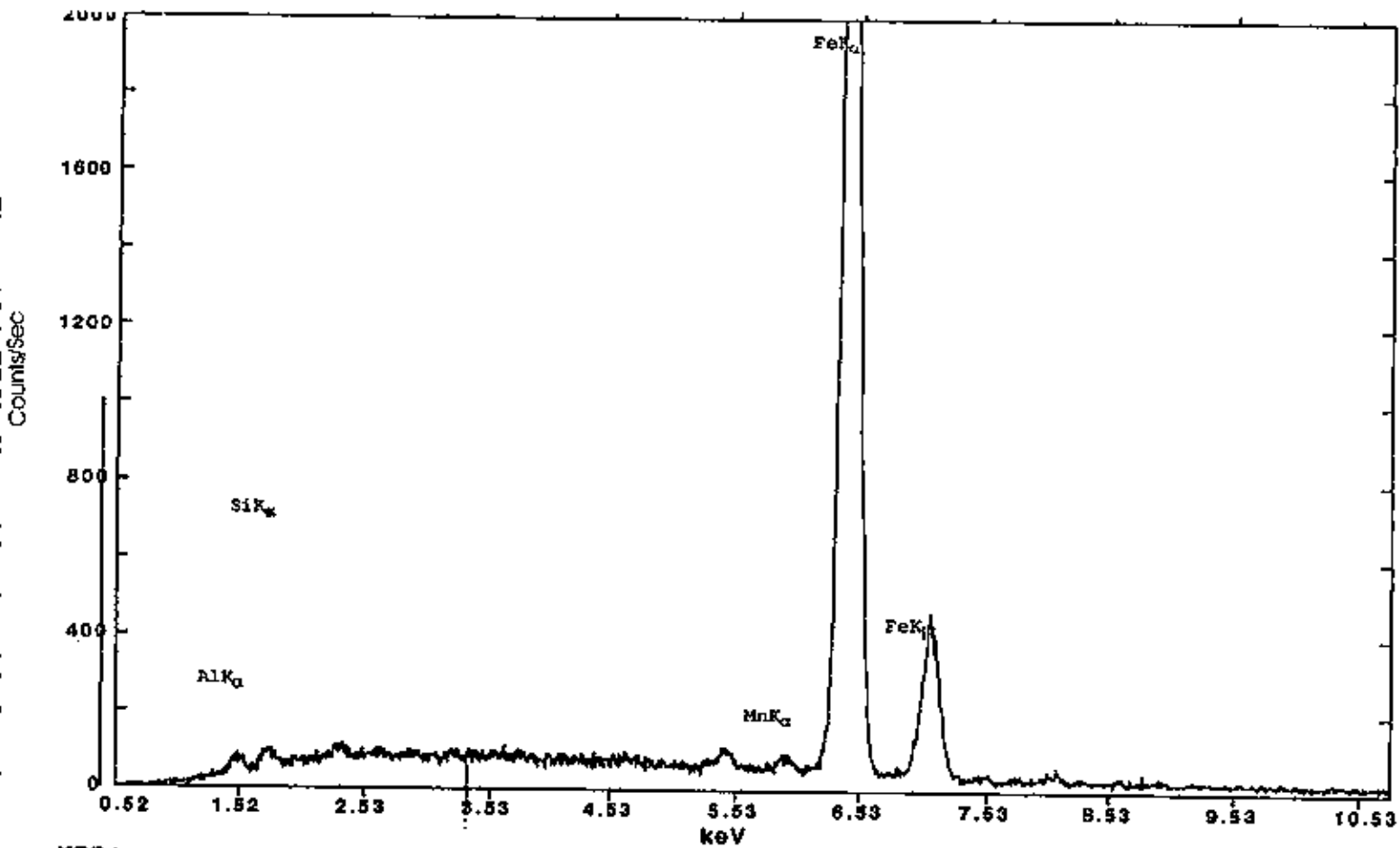
Table A2.2 Horizon description data for non-magnetic core (cont.)

APPENDIX 3: ENERGY DISPERSIVE X-RAY PLOTS

Figure A3.1: EDX of brownish red particle from the magnetically separated material of Profile 2, C→Bw-horizon.	117
Figure A3.2: EDX of iron rich particles from the magnetically separated material of Profile 2, C→Bw-horizon.	118
Figure A3.3: EDX of dome-shaped particle from the magnetically separated material of Profile 2, C→Bw-horizon (Plate 2, Picture 4).	119
Figure A3.4: EDX of the magnetically separated material of Profile 3, A-horizon.	120
Figure A3.5: EDX of the magnetically separated material removed from magnetic core, 39 ft deep.	121
Figure A3.6: EDX of bulk soil removed from the magnetic core, Profile 1, A-horizon.	122
Figure A3.7: EDX of iron rich fragments from the bulk soil from Profile 2, A-horizon.	123
Figure A3.8: EDX of silica rich fragments in the bulk soil from Profile 2, C→Bw-horizon.	124
Figure A3.10: EDX of root in bulk soil removed from an apparent C→Bw-horizon of the nonmagnetic core.	126
Figure A3.11: EDX of tan-white fragments removed from the bulk soil of nonmagnetic core.	127

Figure A3.12: EDX of magnetically separated material removed from the magnetic core, Profile 2, C→Bw-horizon, silt and clay fraction.....	128
Figure A3.13: EDX of bulk soil removed from the magnetic core, Profile 2, C→Bw-horizon, silt and clay fraction.....	129
Figure A3.14: EDX of bulk soil removed from the nonmagnetic core, silt and clay fraction.....	130

Figure A3.1: EDX of brownish red particle from the magnetically separated material of Profile 2, C → Bw-horizon.



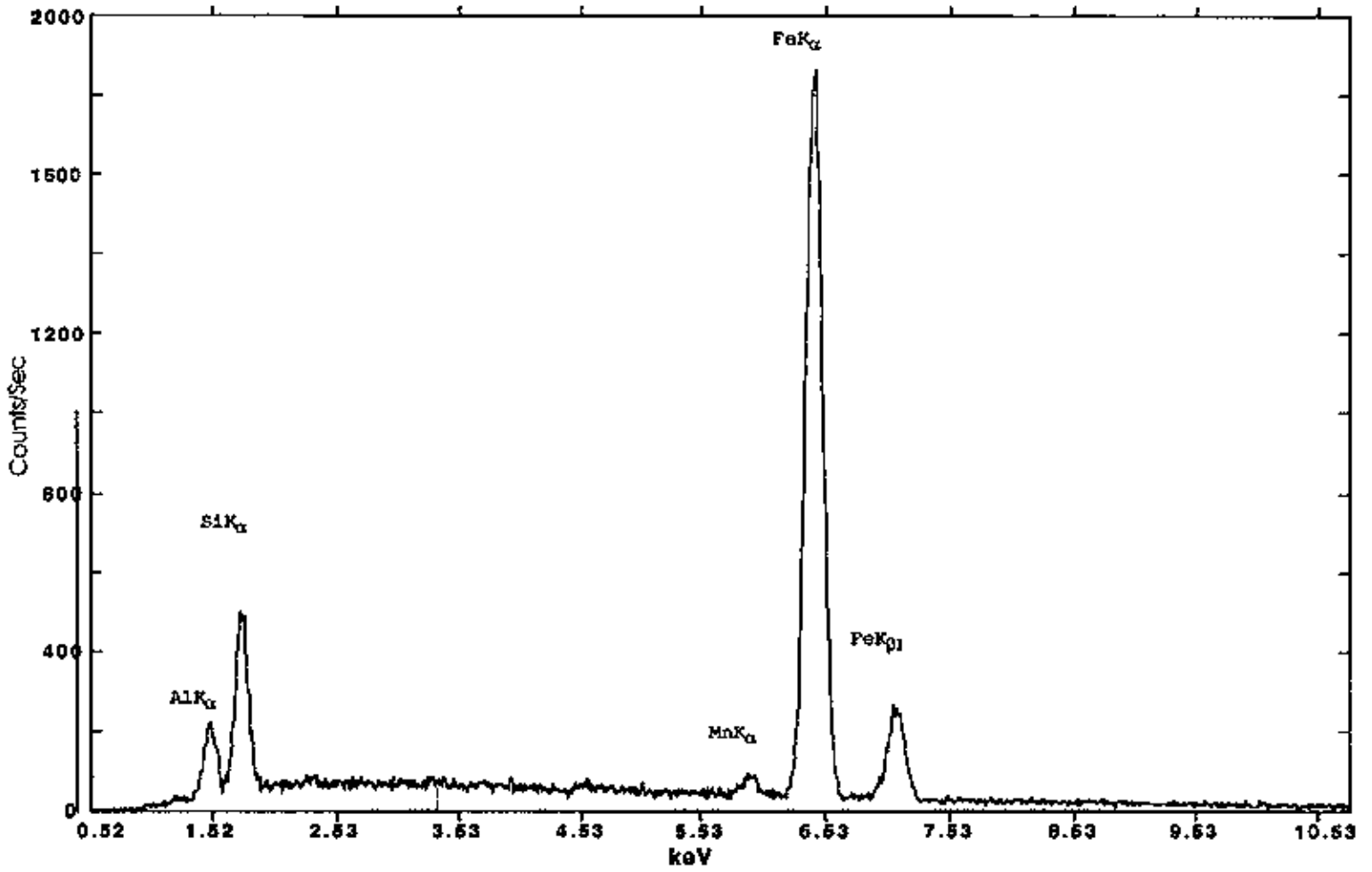
XRD1

XRD1

Analys: Y ROH keV: 20.00 Current: 0.00 Live Time: 100.00 eV/Channel= 10.00

Detector Resolution: 148.19 eV Take-off angle= 40.00 Spectrum # 2 From the file: test Spectrum.Dat

Markers for N. 7



XRD1
XRD1

Analyst: Y ROH keV: 20.00 Current: 0.00 Live Time: 100.00 eV/Channel= 10.00
 Detector Resolution: 146.19 eV Take-off angle= 40.00 Spectrum # 2 From the file: test Spectrum.Dat
 Markers for N : 7

Figure A3.2: EDX of iron rich particles from the magnetically separated material of Profile 2, C \rightarrow Bw-horizon.

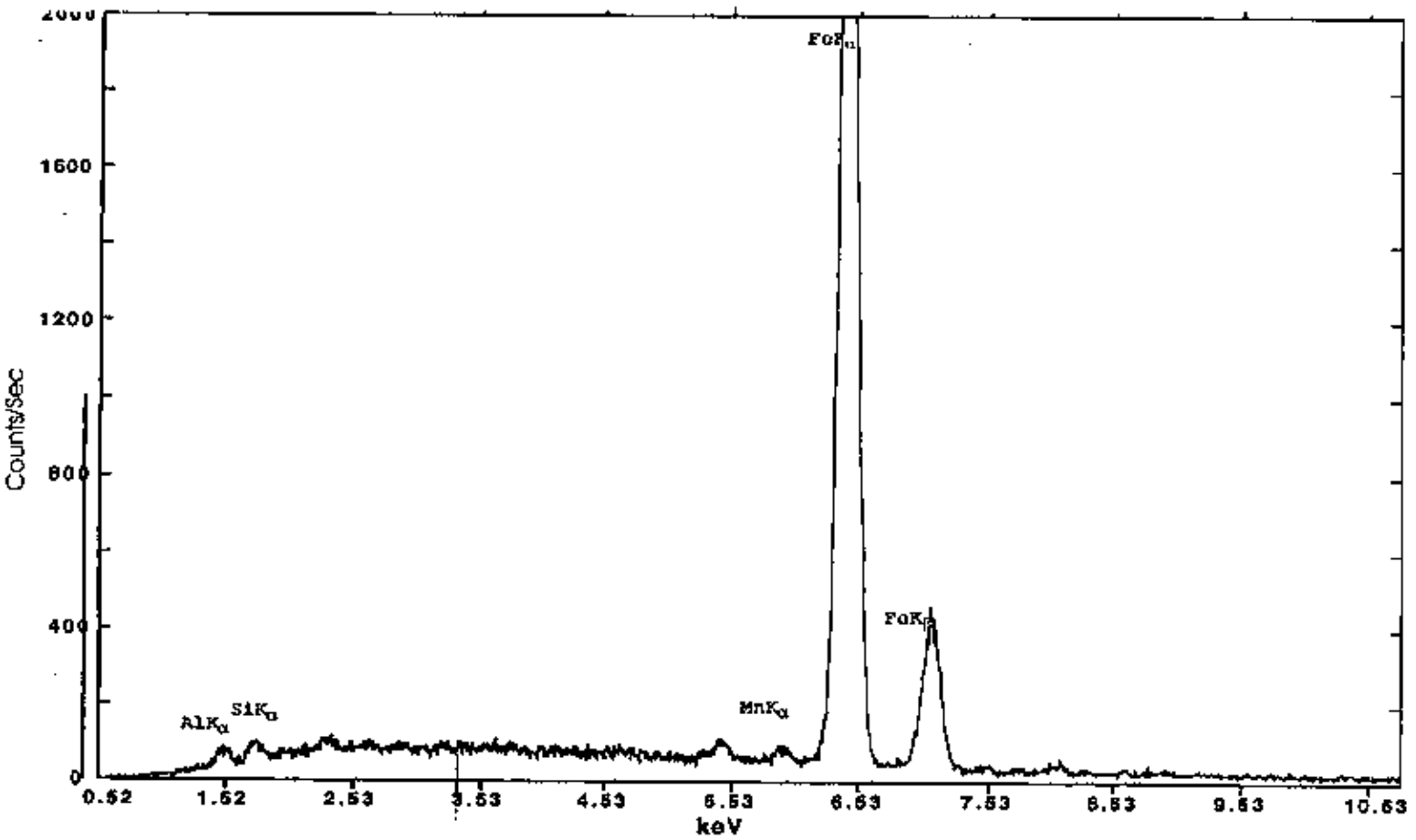


Figure A3.3: EDX of dome-shaped particle from the magnetically separated material of Profile 2, C→Bw-horizon (Plate 2, Picture 4).

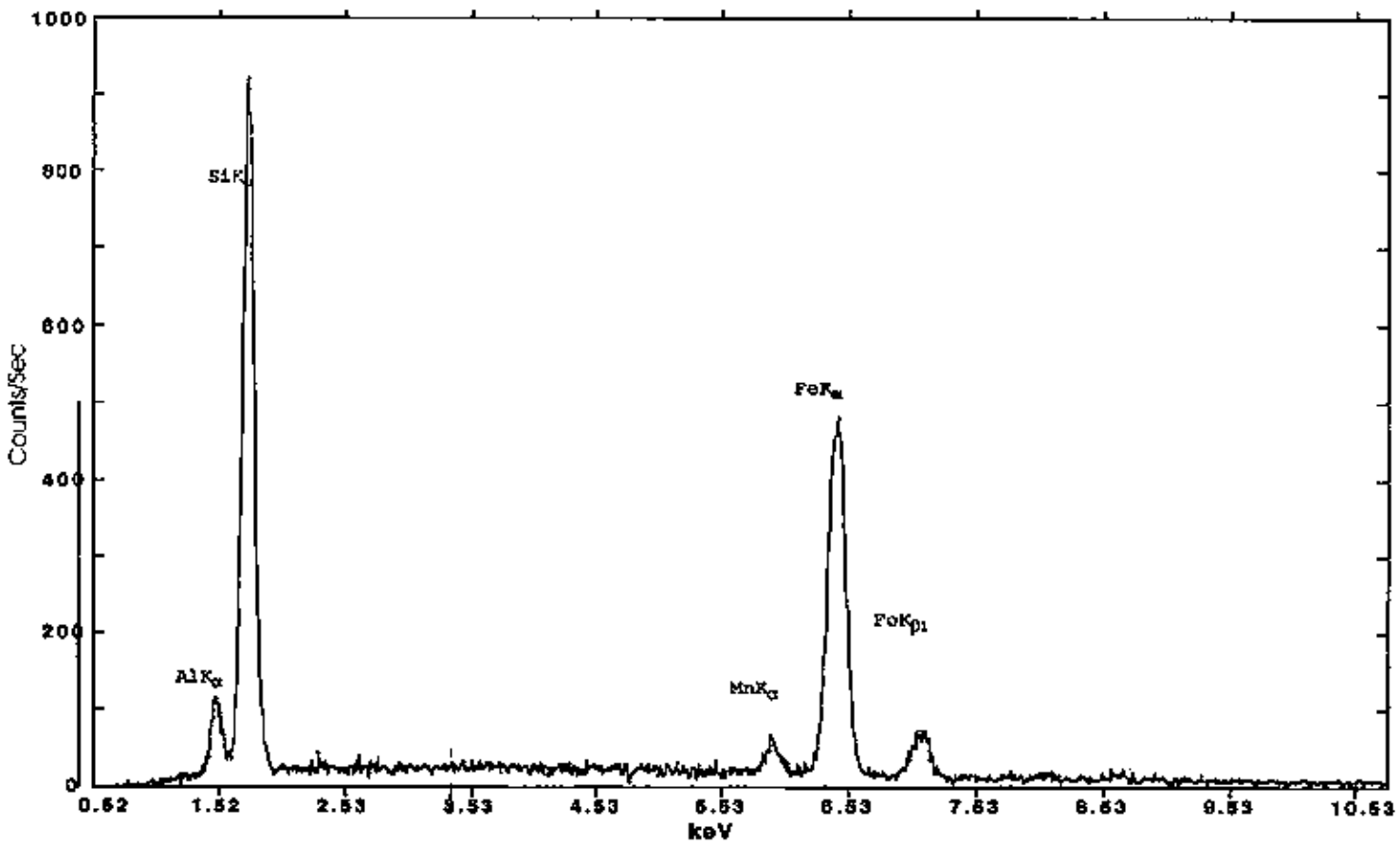


Figure A3.4: EDX of the magnetically separated material of Profile 3, A-horizon.

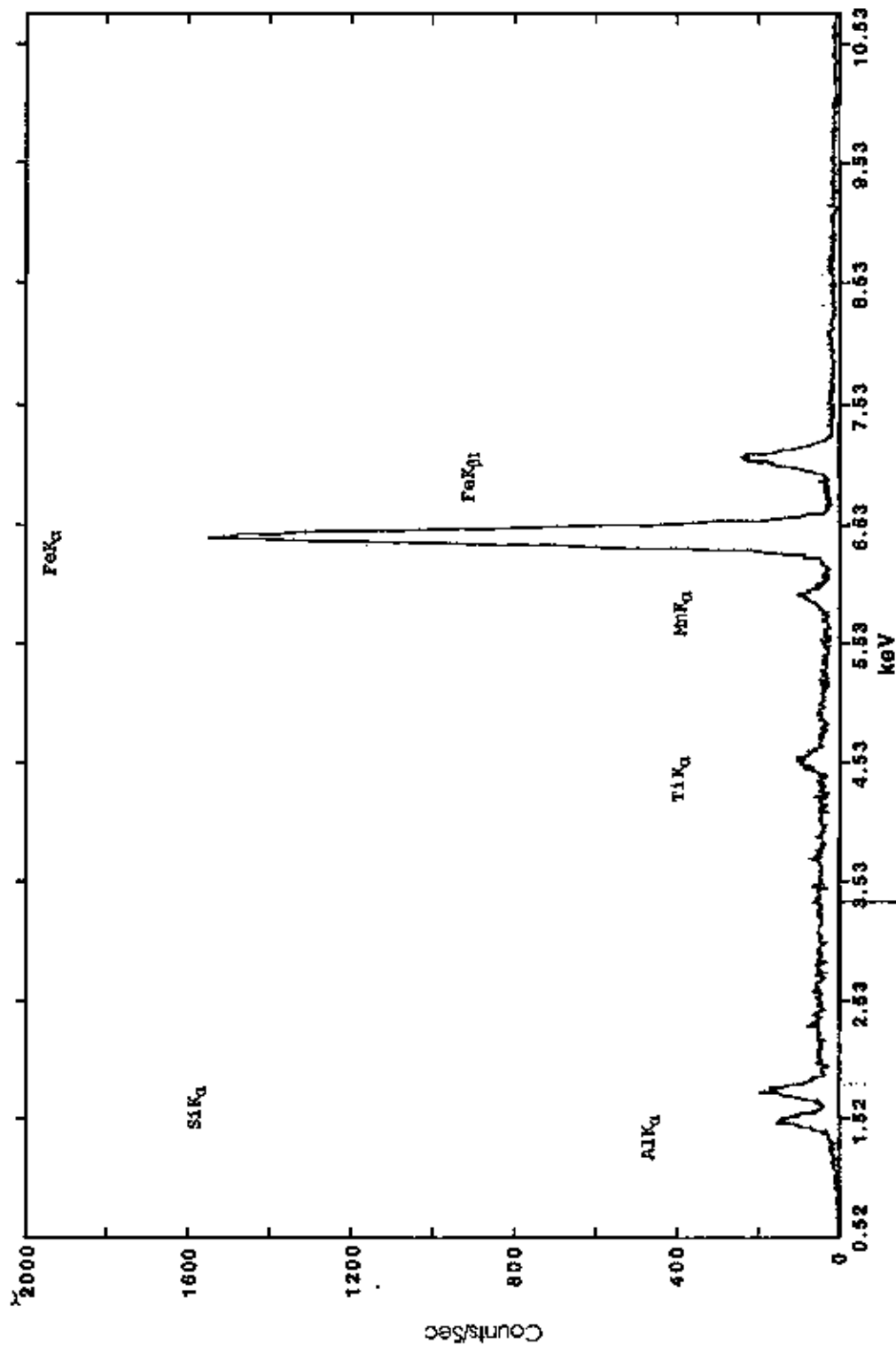


Figure A3.5: EDX of the magnetically separated material removed from magnetic core, 39 ft deep.

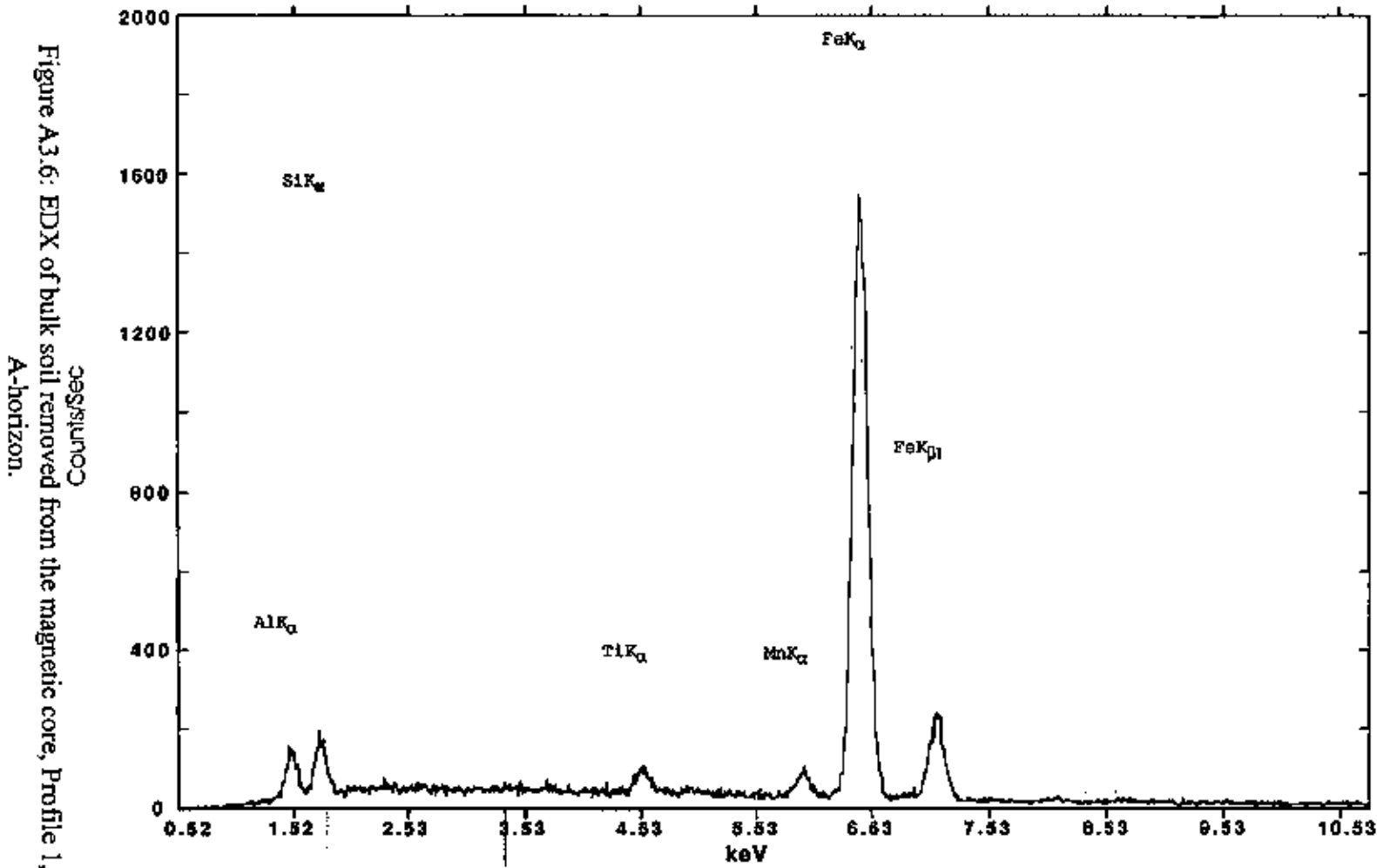


Figure A3.6: EDX of bulk soil removed from the magnetic core, Profile 1, A-horizon.

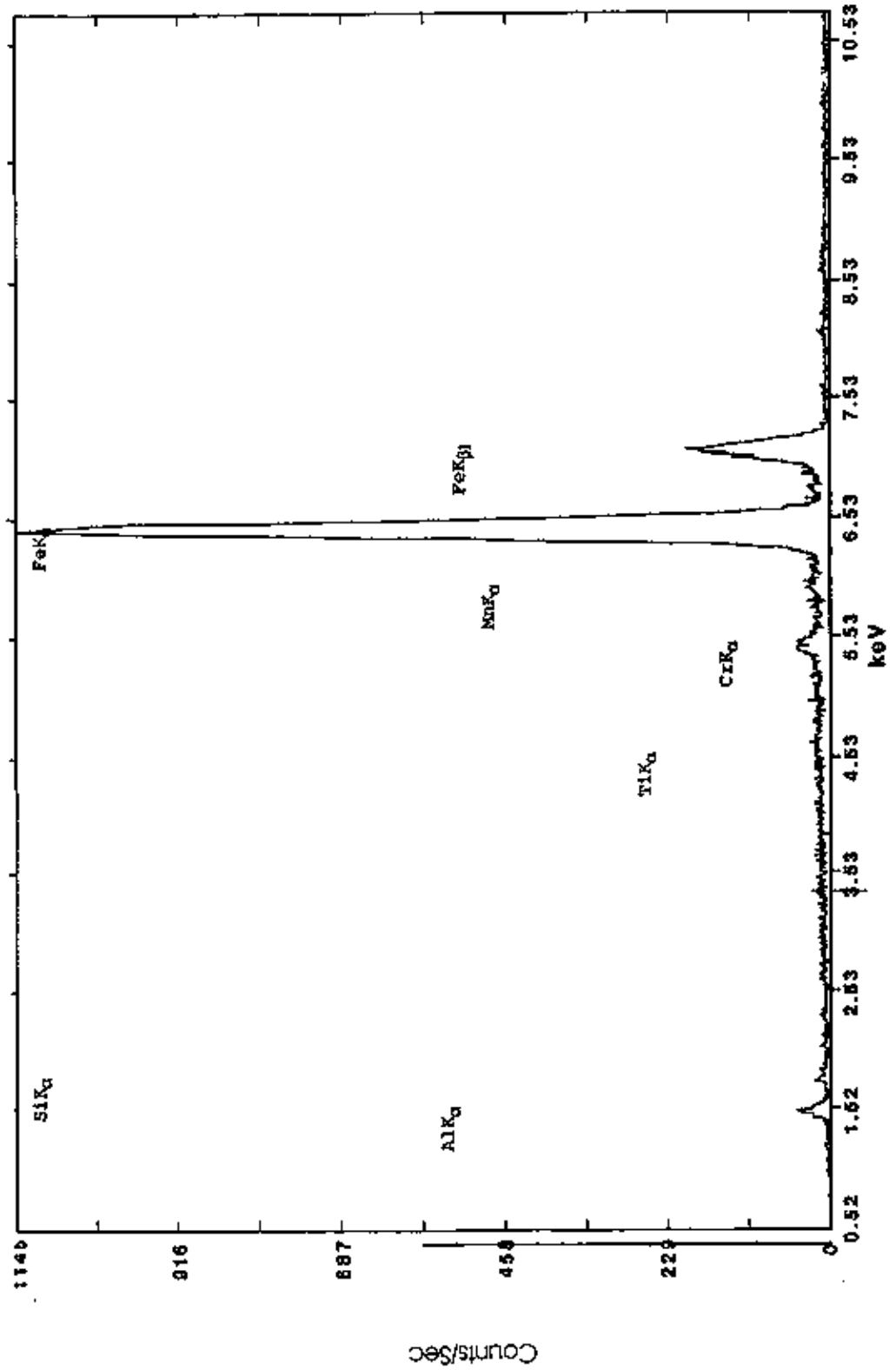


Figure A3.7: EDX of iron rich fragments from the bulk soil from Profile 2, A-horizon.

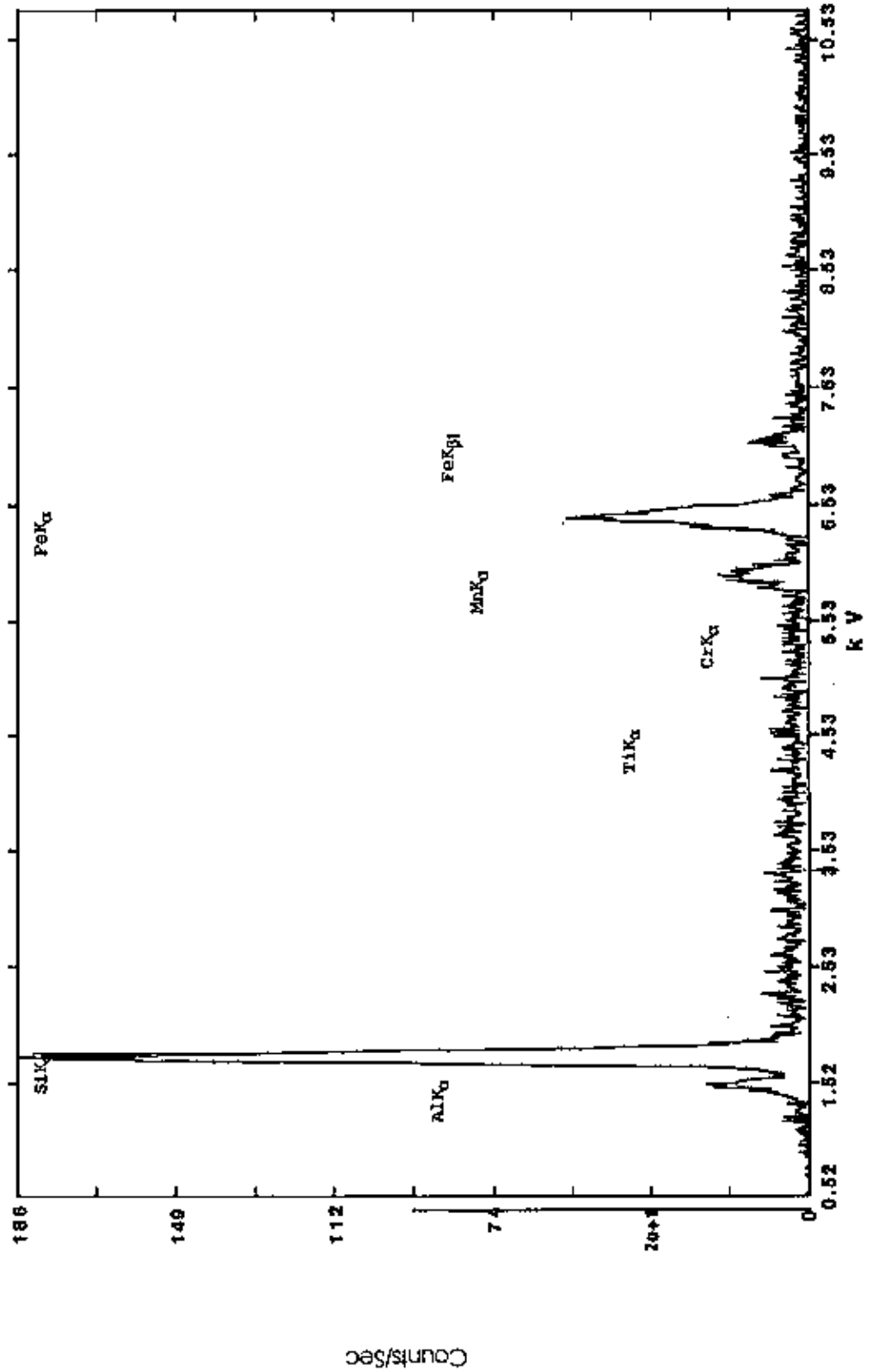


Figure A3.8: EDX of silica rich fragments in the bulk soil from Profile 2, C→Bw-horizon.

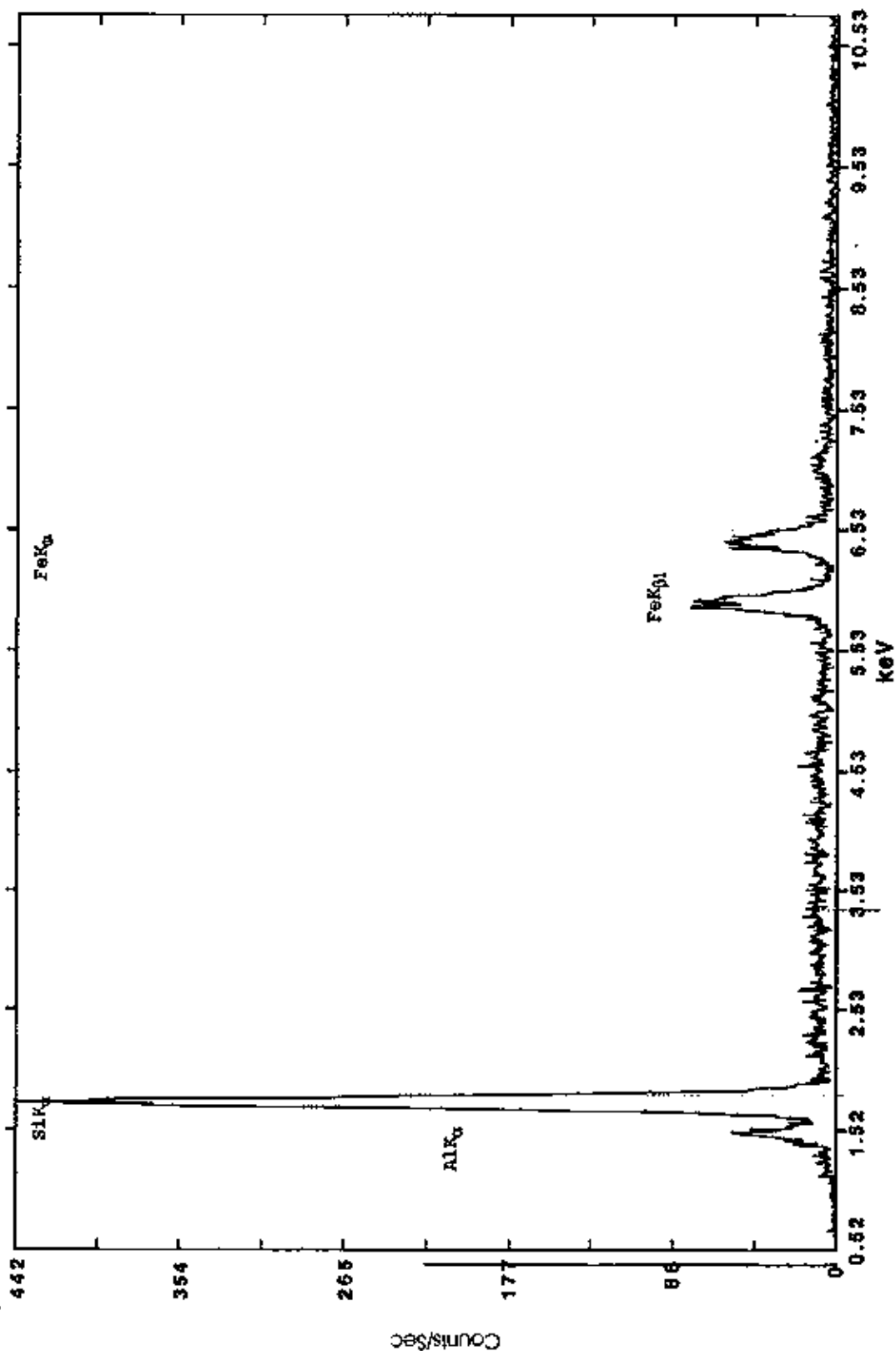


Figure A3.9: EDX of silica rich fragments in bulk soil removed from the magnetic core 39 ft deep.

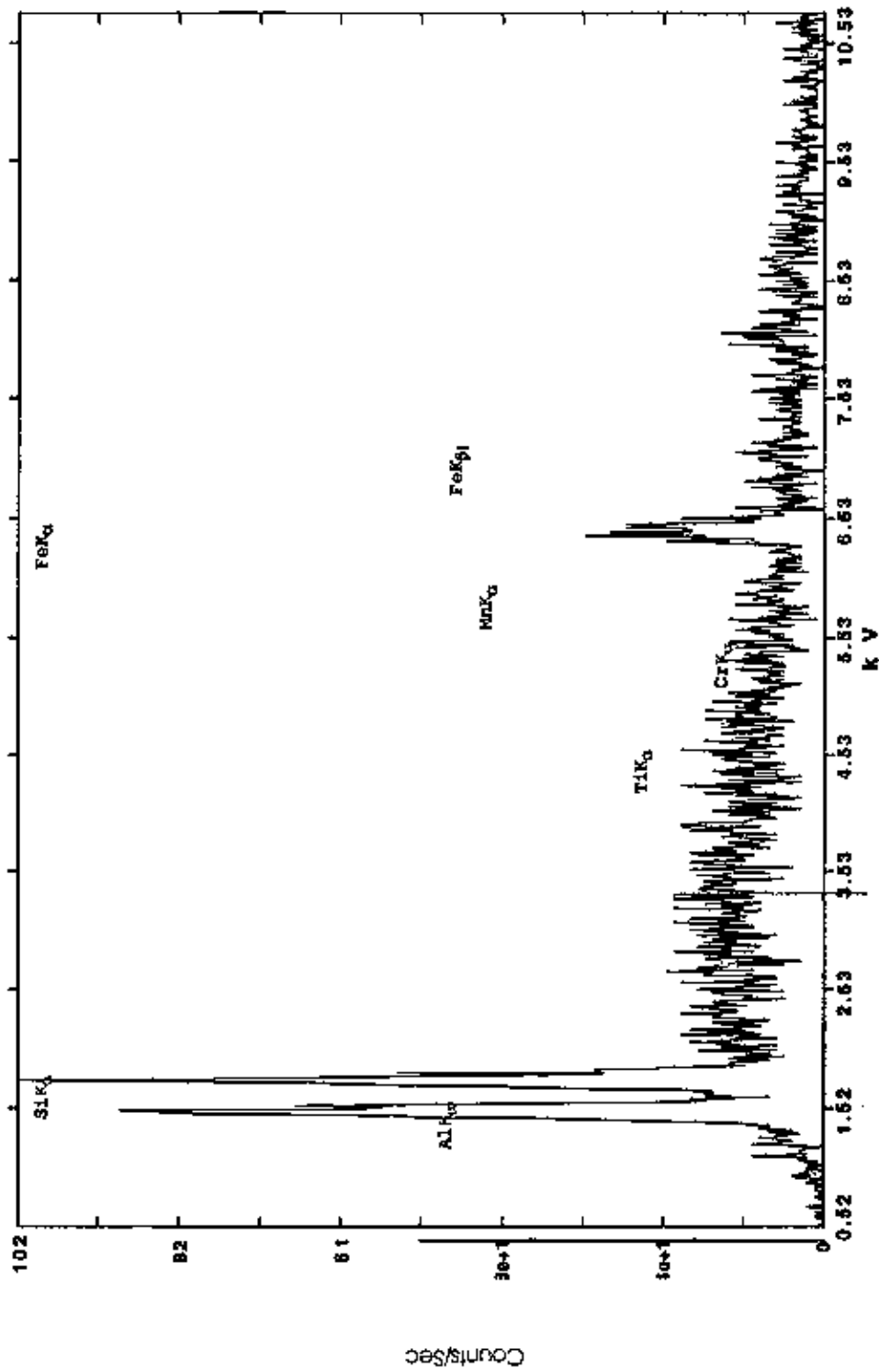


Figure A3.10: EDX of root in bulk soil removed from an apparent C→Bw-horizon of the nonmagnetic core.

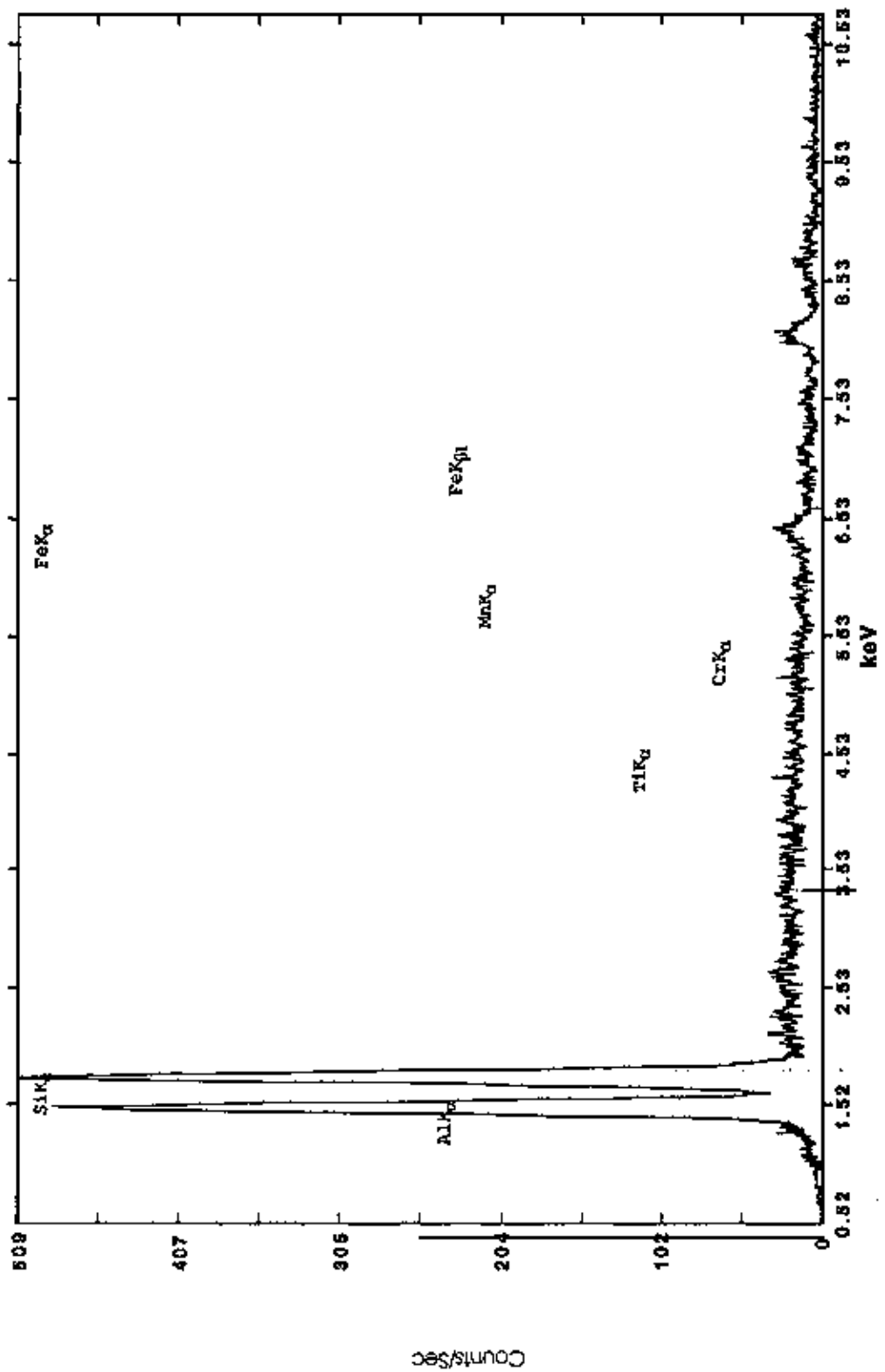


Figure A3.11: EDX of tan-white fragments removed from the bulk soil of nonmagnetic core.

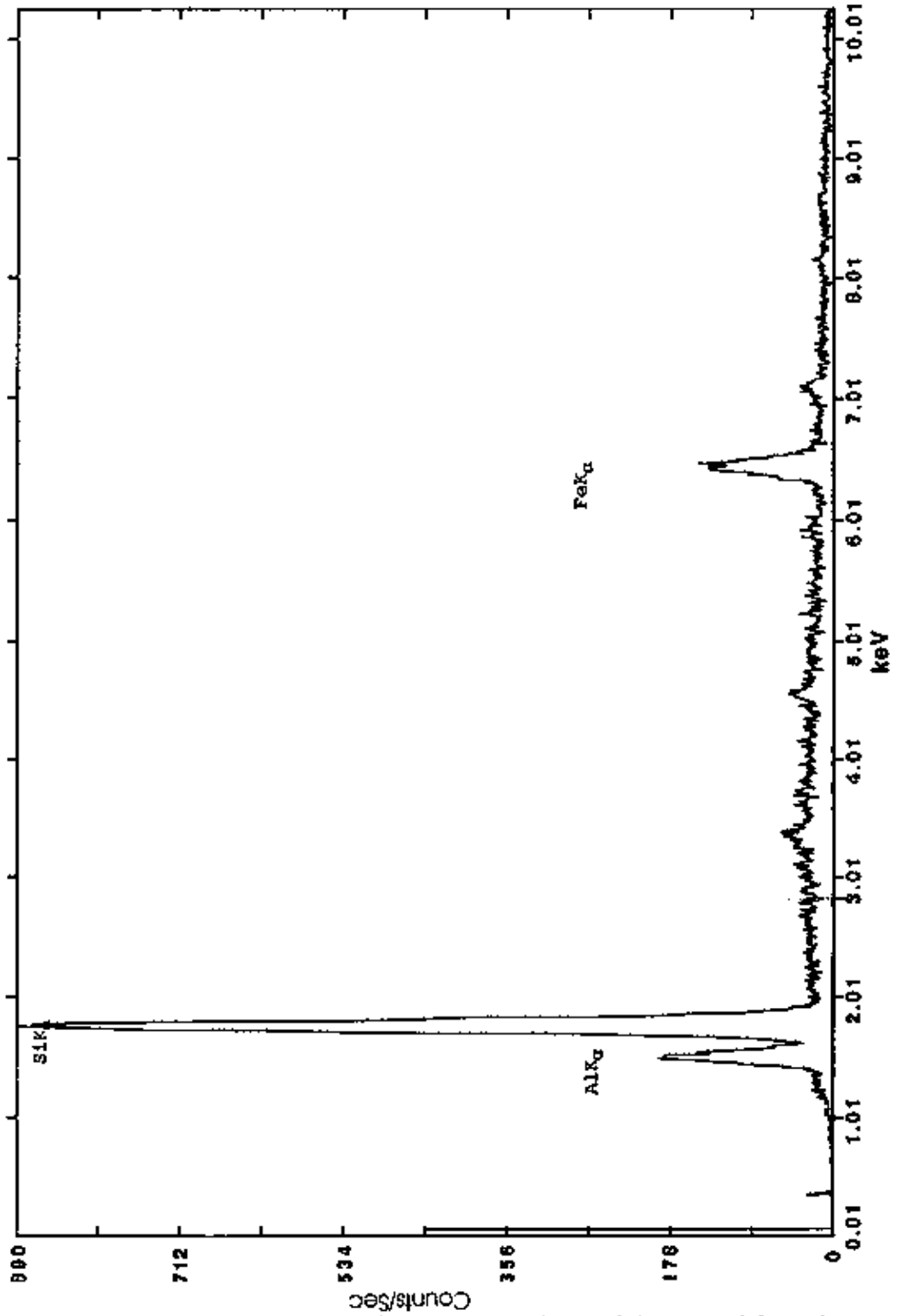


Figure A3.12: EDX of magnetically separated material removed from the magnetic core, Profile 2, C→Bw-horizon, silt and clay fraction.

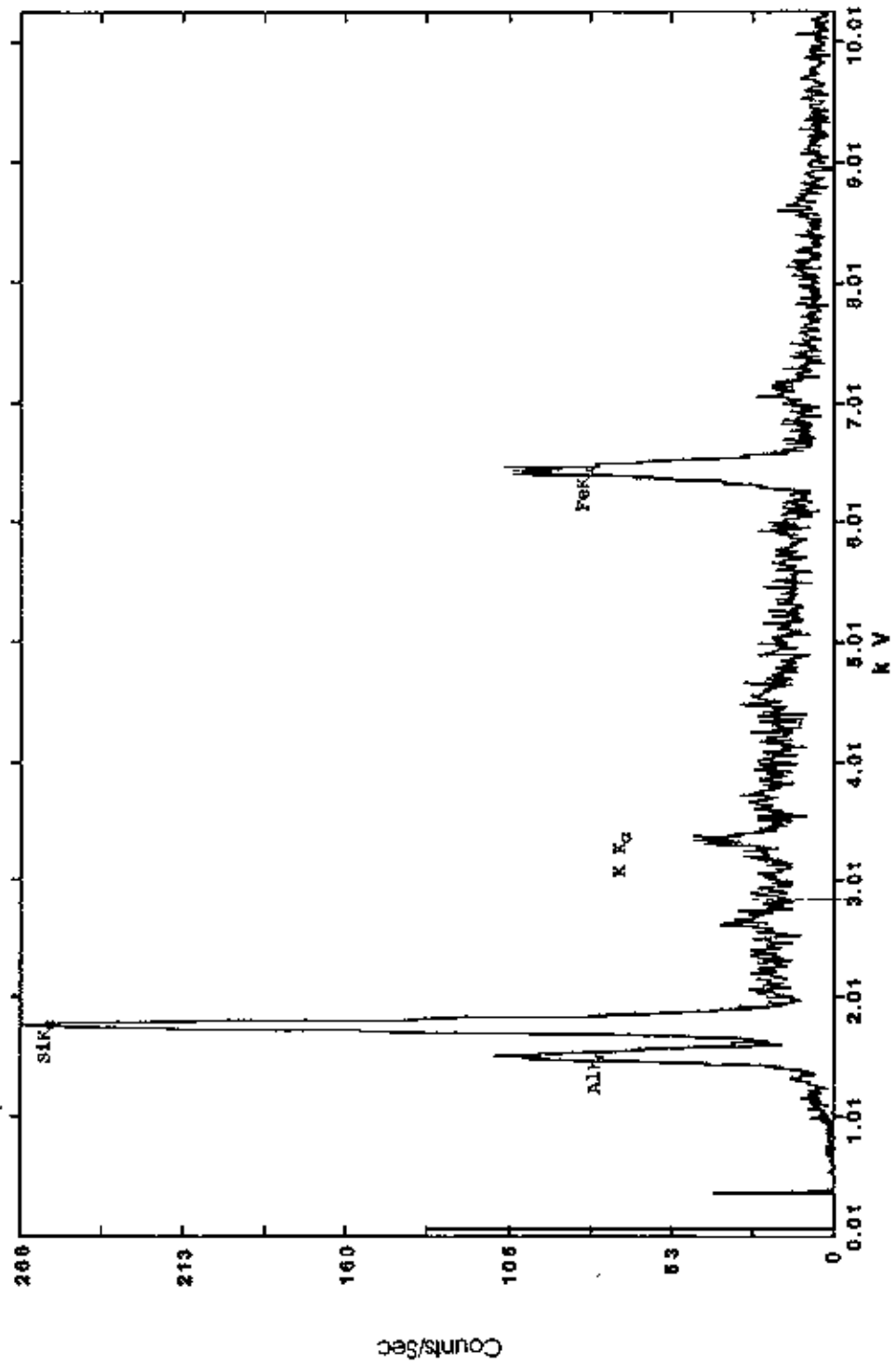


Figure A3.13: EDX of bulk soil removed from the magnetic core, Profile 2, C→Bw-horizon, silt and clay fraction.

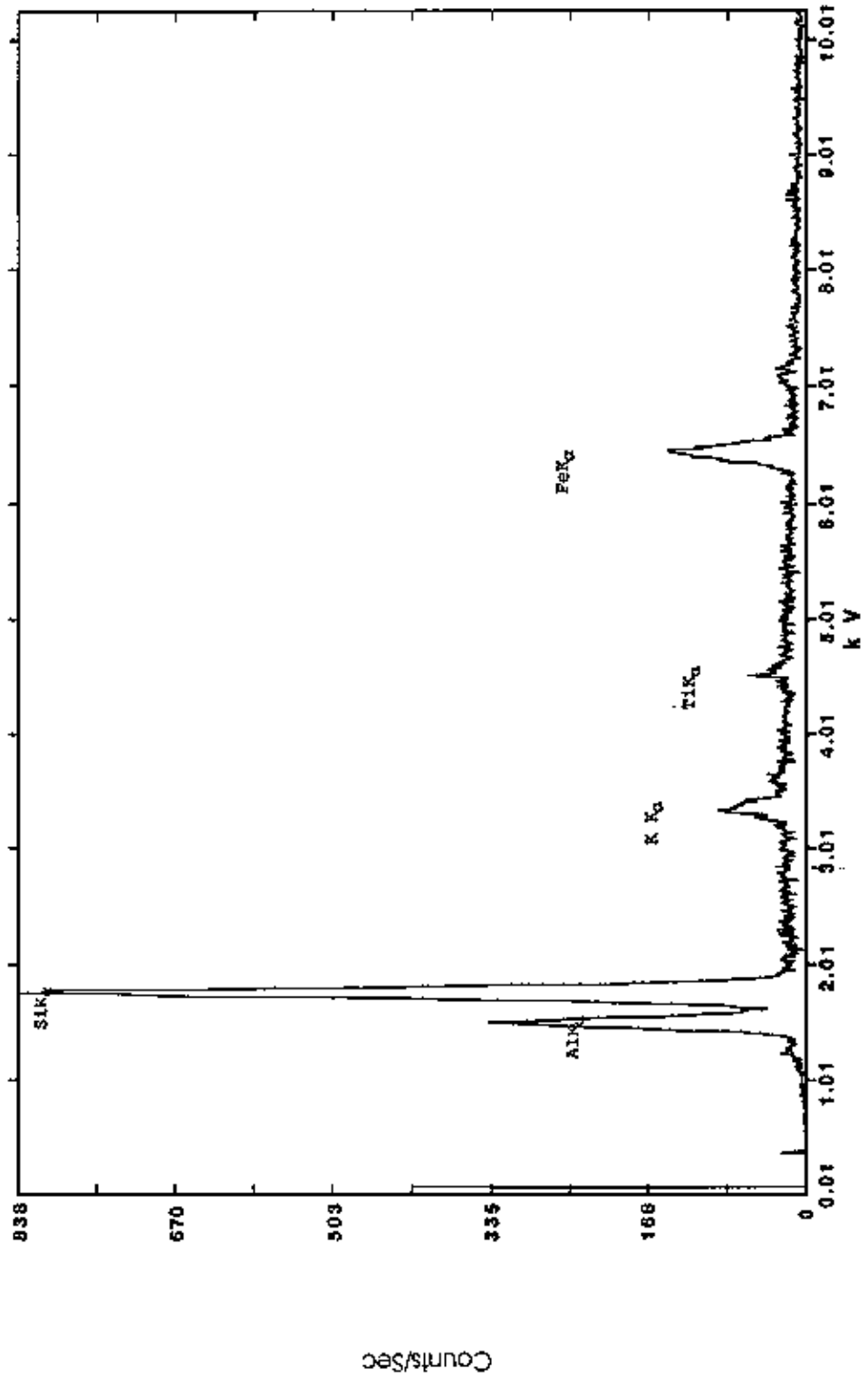


Figure A3.14: EDX of bulk soil removed from the nonmagnetic core, silt and clay fraction.

APPENDIX 4: SOCIETY OF EXPLORATION

GEOPHYSICISTS EXTENDED ABSTRACT

John M. Rivers, Jonathan E. Nyquist, Dennis O. Terry, Jr., and William E. Doll, 2002, Investigations into the origin of magnetic soils on the Oak Ridge Reservation, Oak Ridge, TN: To be published as an extended abstract in the proceedings of the annual meeting of the Society of Exploration Geophysicists.

Investigations into the origin of magnetic soils on the Oak Ridge Reservation, Oak Ridge, TN

John M. Rivers, Jonathan E. Nyquist, Dennis O. Terry, Jr., Temple University; William E. Doll, Oak Ridge National Laboratory*

Summary

In 1993-4, researchers at Oak Ridge National Laboratory collected high-resolution airborne geophysical data on the Oak Ridge Reservation, Tennessee (Doll et al., 2000). The data were collected in part to address concerns about possible undocumented hazardous waste sites. Interpretation of the aeromagnetic data was complicated, however, by the discovery of numerous small magnetic anomalies of natural origin. Magnetic susceptibility measurements made on core showed that the underlying Copper Ridge Dolomite is non-magnetic. Apparently, the magnetic anomalies were created by colluvial infilling of dolines with soil rich in maghemite. We discuss explanations offered in the literature for the formation of magnetic soils, and present evidence based on soil analysis, thin sections, x-ray diffraction, and scanning electron microscopy, that in this case maghemite formed either by anaerobic microbial iron reduction followed by the formation of single-domain maghemite, or by abiological weathering and reduction of an iron-bearing mineral followed by oxidation.

Introduction

In 1993-94, the U. S. Department of Energy (DOE) commissioned an airborne magnetic and electromagnetic survey of the 36,000 acre (14,300 hectare) Oak Ridge Reservation (ORR), located near Oak Ridge, TN. The federal government annexed this land during WWII as part of the Manhattan Project. Nuclear waste and contaminated materials generated in the race to develop a nuclear bomb were typically discarded in shallow waste trenches on the ORR, a practice continued after the war. Ultimately, the EPA designated the ORR a Superfund site, with clean-up responsibility falling on the DOE.

Much of the ORR is undeveloped, originally purchased to create a buffer zone between the nuclear facilities and the surrounding communities. The purpose of the airborne geophysical survey (including radiation, magnetic and electromagnetic sensors, Doll et al., 2000) was to gather geologic information to support hydrologic modeling, and to ensure that no waste areas were overlooked during the clean up.

The resulting aeromagnetic data set revealed large magnetic anomalies over known waste disposal areas and industrial facilities (Nyquist et al., 1996), and numerous magnetic bull's-eye anomalies over smaller metallic targets, such as one-lane bridges, abandoned sheds, power line towers, cars and trucks (Nyquist and Beard, 1996).

Some of the bull's-eye anomalies were of natural origin. Helm (1995, unpublished) showed that all three groups of the ORR bedrock (Conasauga, Knox and Chickamauga) have weak magnetic susceptibility, averaging below 50×10^{-5} S.I. Nonetheless, follow-up field investigations led to the discovery of pockets of highly magnetic soil (Doll et al., 1995). The Copper Ridge dolomite, which occurs on the ridge tops and underlies the magnetic soils, has an average magnetic susceptibility of only 5.0×10^{-5} S.I. Oak Ridge researchers collected soil cores and surface magnetic data over some of these anomalies, but investigation into the origin of these magnetic soils was not a high priority with DOE.

Driven by scientific curiosity, we have returned to this problem. Geophysicists are keenly aware that magnetic soils can be a source of geologic noise. When collecting surface magnetic data, for example, the sensor is typically mounted on a non-magnetic pole a couple of meters above the ground surface, sacrificing some resolution to minimize the influence of variations in soil magnetic susceptibility. Deep pockets of magnetic soils tens of meters across are less common, however, and alarming when the goal is to sift through a large magnetic data set in search of small, forgotten caches of buried drums.

Previous Investigations

Some soils on the ORR contain maghemite (Lee et al., 1984; Hatcher et al., 1992; Kopp and Lee, 1987). These soils are paleudults (old ultisols) and referred to as ancient alluviums (late Tertiary). Evidence of their age includes highly weathered and iron-oxide-impregnated chert fragments. Clues to past alluvial (river) influence include occasional rounded metaquartzite cobbles. These soils are found on Copper and Chestnut ridge tops as a result of topographic inversion. Yet soil maps (Lietzke, 1994) do not show precise correlation between

Magnetic Soils

the ancient alluviums and the magnetic anomalies.

Doll and Kaufmann (unpublished) chose a large soil anomaly for further study. They collected soil cores and measured the magnetic susceptibility using a Bartington MS2 meter with a 80mm-diameter MS2C core sensor. They found that the soil in a magnetic bull's-eye had a magnetic susceptibility as high as 400×10^{-5} S.I. in the upper two feet, and a susceptibility greater than 100×10^{-5} S. I. to a depth of more than 50 feet. A shorter, 15-ft core taken outside of the anomaly had a magnetic susceptibility less than 50×10^{-5} S.I. over its entire length.

Methods

We photographed each 2-ft section of soil core and documented ped structure, horizon changes, wet/dry color, mineralogy, roots, thin section removal areas, and areas from which scanning electron microscope (SEM) and x-ray diffraction (XRD) samples were taken. We also verified the magnetic susceptibility measurements made previously by Doll and Kaufmann. Horizon intervals were designated and horizons described and documented. We selected soils for thin sectioning based on the nature of the horizon changes and the magnetic susceptibility data.

We extracted magnetic soil components from the core intervals with the highest magnetic susceptibility using a horseshoe magnet and characterized the mineralogy by XRD using a Scintag XDS 2000 diffractometer operating at a scan rate of 2° 2θ /min. Cobalt K- α radiation ($\lambda = 1.79026\text{\AA}$) was used for the XRD analyses.

We used a JEOL JSM-350F SEM to examine mineral grains prepared from both the magnetic and non-magnetic soil cores, photograph the grains, and evaluated the chemistry of the particles using energy dispersive x-ray (EDX). The purpose the SEM and EDX work was to determine whether the magnetic particles in the soil were of biologic or abiologic origin.

Results and Discussion

The XRD work confirmed that the mineral maghemite is responsible for the high magnetic

susceptibility of the ORR soils. Soil recovered from inside the magnetic anomaly had an average susceptibility of 251×10^{-5} S.I. while the soil from outside the anomaly had an average susceptibility of 19×10^{-5} S.I.

Figure 1 shows susceptibility of the soil column collected inside the magnetic anomaly and the pedology based on inspection and thin section analysis. Analysis revealed multiple buried soil profiles. Susceptibility peaks in both cores were associated with the transition from the A to the B/C horizon.

The XRD work showed that the soils are rich in quartz, contain the clay mineral kaolinite, and have been highly leached. The magnetic soil also contained some illite, a diagenetic product of biotite, which implies a source other than dolomite. It appears that the soils from both inside and outside the magnetic anomaly are products of colluvium washed down from the top of Copper Ridge. Strong magnetic anomalies formed where this magnetic soil collected in dolines. The parent material is old enough to have begun the process of kaolinizing chert (converting to clay), a material very resistant to weathering. This supports the hypothesis that ancient alluvium was the source of the colluvium.

Evaluating the Theories of Magnetic Soil Formation

Numerous mechanisms have been proposed in the literature for the genesis of magnetite (which readily oxidizes to maghemite) in soils. On the basis of our work, most can be ruled out for the magnetic soils on the ORR. The following is based on a list given by Dearing (1996).

1) Long term weathering and pedogenesis that concentrates primary residual ferrimagnetic minerals. Helm (1995) showed the underlying rock to be nonmagnetic, so it is unlikely that iron in the dolomite is in a highly magnetic form. This interpretation is supported by Moukarika et al. (1991) who studied magnetic soils formed on dolomite. They determined that the dolomite supplied the iron to the magnetic soil in the form of hematite and goethite but that the soil magnetism was due to later transformation of these oxides into maghemite. The possibility of magnetic enhancement of the soil due to the

Magnetic Soils

weathering of a magnetic parent material can be rejected.

2) *Accumulation of relatively coarse (>1 μm) airborne magnetic particulates mainly from pollution sources.* Typical fly ash is on the order of 1 μm (Tompson and Oldfield, 1986; King, 1999) and in study of particulate samples in the United Kingdom. King et al. (1999) showed the largest particulates of any kind found were 190 μm. The pure FeO particles imaged using SEM (Figure 2) are 200-2500 μm, which is too large to be fly ash.

3) *Strictly anaerobic bacteria that produce single domain magnetite (Fe₃O₄) grains with diameters <50nm.* The two pure iron oxide particles located using SEM were far too large to be produced by this mechanism (Figures 2). The roundness of these particles does not fit the description of magnetite produced by magnetotactic bacteria. These are usually cubic, octahedral and more rarely prismatic, tooth-shaped, arrowhead-shaped and bullet-shaped. Rounded forms are rare and associated with smaller than average magnetotactic crystals (Devouard et al., 1998).

4) *Anaerobic formation of greigite (Fe₃S₄) linked to microbial reduction.* Stanjek et al. (1994) show greigite to form at a depth of 2.5 feet in a gley (reduced) soil as a result of sulfate reduction due to anaerobic respiration. Magnetic enhancement on the ORR is associated with oxidized horizons. In Stanjek's study, sulfate was supplied by pyrite in the parent rock of the soil. Pyrite has not been reported in the underlying dolomite. Most importantly, we have shown that maghemite is the principal magnetic mineral on the ORR.

5) *Microaerophilic assimilatory bacteria (magnetotactic bacteria) that produce chains of single-domain magnetite magnetosomes with diameters 100-220nm.* Again, the magnetic iron oxide particles located using SEM (Figure 2) are too large and too rounded to support this theory. Furthermore, these bacteria thrive in reducing conditions, whereas the highest magnetic signal in these soils is associated with oxidized horizons.

6) *Thermal transformation of weakly magnetic iron oxides and hydroxides to ferrimagnetic magnetite or maghemite by natural fires or crop burning in the presence of organic matter.* The depth and distribution of the magnetic signal would not seem to support this process. First, if fire caused the magnetism we would expect magnetic soils to be ubiquitous, not confined to the bull's-eye pattern seen on the ORR. The depth of the magnetic soils (>50 ft) also argues against this possibility.

7) *Fulgurites (formations caused by lightning strikes).* We would expect the fulgurite (lightning) mechanism to create bull's-eye anomalies but we would not expect any magnetic transformation caused by a single strike to extend more than 50 ft deep. To explain the susceptibility peaks in the soil core lightning would have to strike the low-lying dolines before each subsequent burial. Furthermore, the vesicular glass relicts created by the fusing of silica during lightning strikes were not seen in the thin sections.

Two hypotheses remain viable after our analysis.

They are:

8) *Anaerobic microbial Fe reduction followed by formation of single-domain magnetite or maghemite (γ-Fe₂O₃) grains with diameters <100nm.*

Or

9) *Abiological weathering of the Fe(III) bearing minerals followed by oxidation leading to magnetite or maghemite, as demonstrated in synthetic experiments (Taylor et al, 1987).* One or both of these mechanisms is most probably responsible for the magnetic enhancement of soils on the ORR. Magnetite contains ferric (oxidized) and ferrous (reduced) iron. Both 8 and 9 can create maghemite through cycles of reduction followed by oxidation. The only difference between the mechanisms is the reducing agent. In one case the reducing agent is microbial, and in the other it is abiological (water table fluctuations). Because the morphology and size of the magnetic particles created by these two mechanisms are similar, it is not possible to ascertain which mechanism is most responsible for the magnetic enhancement of the soil on the ORR.

Out of 14 profiles identified in the two soil cores, 10 showed increased magnetic susceptibility at the bottom of the A-horizon. This susceptibility pattern seen in the cores is a reflection of the cyclic redox environment optimal for the creation of maghemite. The spikes are evidence of relict redox boundaries of now buried soils.

Conclusions

According to soil maps and the Status Report on the Geology of the Oak Ridge Reservation (Hatcher, 1992), the parent material of the

Magnetic Soils

magnetic soil is ancient alluvium found at the crest of the Copper Ridge. Support for this interpretation is found in the quartzite grain located in a thin section taken from the soil. According to Phillips et al. (1998), cobbles of metaquartzite are evidence of ancient alluviums that were deposited by rivers that flowed from the Unaka Mountains or the Clinch Mountain. How much of the magnetic soil in the core is original alluvium and how much is Copper Ridge residuum is unclear, but undoubtedly the two mixed during colluviation.

The alluvium-associated magnetic soil is richer in iron than the soil from outside of the anomaly. This can be seen in EDX data, which shows iron to be the second most abundant element in the silt and clay fraction of the magnetic soil and the third (after aluminum) in the nonmagnetic. The only difference between the two soil histories seems to be the influence of the ancient alluvium that has accumulated in the dolines. The alluvium was probably originally enriched in iron by the weathering of minerals carried by the river from the mountains.

This study illustrates why geophysicists interpreting magnetic data must be mindful of magnetic soils even when the underlying bedrock is non-magnetic, particularly when working in areas where soil may have accumulated in topographic depressions such as dolines.

References

- Dearing, J. A., Hay, L. K., Baban, S. M. J., Huddleston, A. S., Wellington, E. M. H., Loveland, P. J., 1996. Magnetic Susceptibility of soil: an evaluation of conflicting theories using a national data set: *Geophys. J. Int.* v. 127, p. 728-734.
- Devouard, B., Posfai, M., Hua, X., Bazylnski, D. A., Frankel, R. B., Buseck, P. R., 1998. Magnetite from magnetotactic bacteria: size distributions and twinning: *American Mineralogist*, v. 83, no. 11-12, p. 1387-1398.
- Doll, W. E., Helm, J. M., Beard, L. P., 1995. Airborne Detection of Magnetic anomalies Associated with Soils on the Oak Ridge Reservation, Tennessee. Symposium on the Application of Geophysics to Engineering and Environmental Problems, Eng. Environ. Geophys. Soc., p. 619-626.
- Doll, W. E., Nyquist, J. E., Beard, L. P., Gamey, T. J., 2000. Airborne geophysical surveying for hazardous waste site characterization on the Oak Ridge Reservation, Tennessee: *Geophysics*, v. 65, no. 7, p. 1372-1387.
- Hatcher, R.D., P.J. Lemiszki, R.B. Dreier, R.H. Kettle, R.R. Lee, D.A. Leitzke, W.M. McMaster, J.L. Foreman, and S.Y. Lee, 1992. Status report on the geology of the Oak Ridge Reservation, ORNL/TM-12074, 244 p.
- King, A. M., Jones, A. M., Dorling, S. R., Merefield, J. R., Stone, I. M., Hall, K., Garner, D. V., Hall, P. A., Stokes, B., 1999. Study for particulate sampling, sizing and analysis for composition, ETSU N/01/00049/REP, 131 p.
- Kopp, O.C., Lee, S.Y., 1987. An unusual occurrence of maghemite on soils developed on dolostones of the Knox Group, Oak Ridge, Tennessee, in *Proceedings of the International Clay Conference*, Denver, The Clay Minerals Society, Bloomington, Indiana, p. 205-211.
- Lee, S. Y., Kopp, O. C. and Lietzke, D. A., 1984. Mineralogical characterization of West Chestnut soils, ORNL/TM-9361, 85 p.
- Leitzke, D. A., 1994. Soils of Walker Branch Watershed: ORNL/TM-11606, 107 p.
- Moukarika, A., O'Brien, F., Coey, J. M. D., Resende, Mauro, 1991. Development of magnetic soil from ferroan dolomite: *Geophysical Research Letters*, v. 18, p. 2043-2046.
- Nyquist, J. E., Beard, L. P., and Johnson, D., 1996. Ground and Airborne Magnetic and Electromagnetic Surveys at a Hazardous Waste Site, in: *Case Histories of Geophysics Applied to Civil Engineering and Public Policy*, Geotechnical Special Publication No. 62, Michaels, P., and Woods, R. (eds.), American Society of Civil Engineers, p. 1-13.
- Nyquist, J. E., and Beard, L. P., 1996. Clean enough for industry? An airborne geophysical case study. Symposium on the Application of Geophysics to Engineering and Environmental Problems, Eng. Environ. Geophys. Soc., p. 853-864.
- Phillips, D. H., Ammons, J. T., Lee, S. Y., Lietzke, D. A., 1998. Deep weathering of calcareous sedimentary rock and the redistribution of iron and manganese in soil and saprolite: *Soil Science*, v. 163, p. 71-81.
- Stanjek, H., Fassbinder, J. W. E., Vali, H., Graf, W., 1994. Evidence of biogenic greigite: *Journal of Soil Science*, v. 45, p. 97-103.
- Taylor, M. R., Maher, B. A., Self, P. G., 1987. Magnetite in soils: I. The synthesis of single-domain and superparamagnetic magnetite: *Clay Minerals*, v. 22, p. 411-422.
- Tompson, R., Oldfield, F., 1986. *Environmental magnetism*: London, Allen & Unwin, 227 p.

Acknowledgements

We thank Dr. Yul Roh for his generous assistance with the XRD and SEM analysis. Oak Ridge National Laboratory is managed by UT-Battelle, LLC for the U. S. Department of Energy under contract DE-AC05-00OR22725. The submitted manuscript has been authored by a contractor of the U. S. Government. Accordingly, the U.S. Government retains a nonexclusive, royalty-free license to publish or reproduce the published form of this contribution, or allow others to do so for U. S. Government purposes.

Magnetic Soils

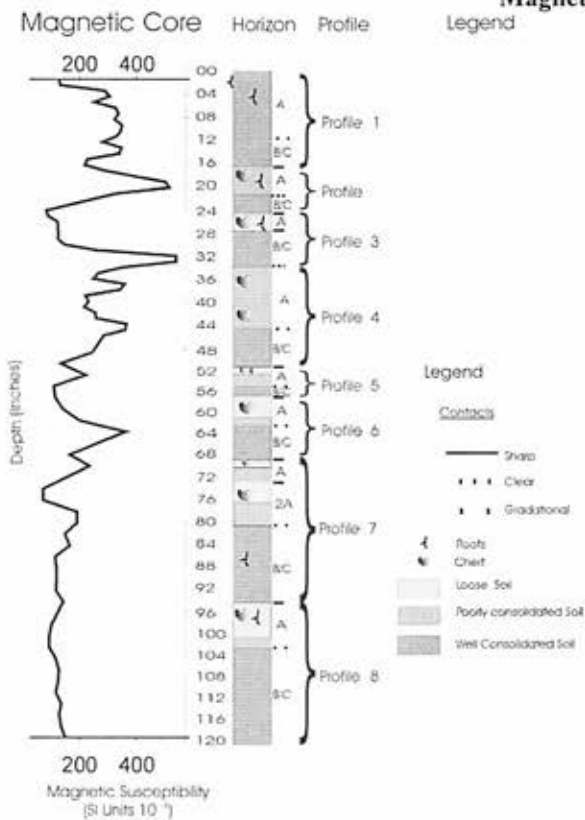


Figure1: Magnetic susceptibility and soil profiles for the core taken within the magnetic anomaly.

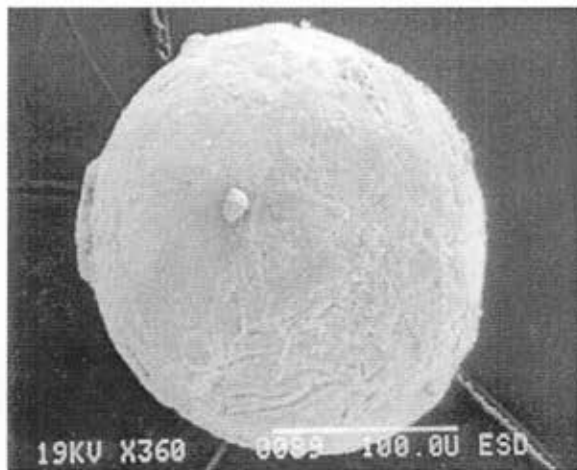


Figure2: SEM image of a magnetic particle separated from the soil core.